

The Dominant Pathways for the Conversion of Methane into Oxygenates and Syngas in an Atmospheric Pressure Dielectric Barrier Discharge

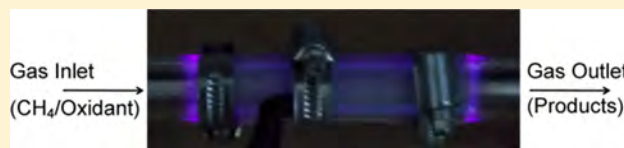
Christophe De Bie,[†] Jan van Dijk,[‡] and Annemie Bogaerts^{*,†}

[†]Research Group PLASMANT, Department of Chemistry, University of Antwerp, Universiteitsplein 1, 2610 Wilrijk-Antwerpen, Belgium

[‡]Department of Applied Physics, Eindhoven University of Technology, Den Dolech 2, Postbus 513, 5600 MB Eindhoven, The Netherlands

S Supporting Information

ABSTRACT: A one-dimensional fluid model for a dielectric barrier discharge in CH₄/O₂ and CH₄/CO₂ gas mixtures is developed. The model describes the gas-phase chemistry for partial oxidation and for dry reforming of methane. The spatially averaged densities of the various plasma species are presented as a function of time and initial gas mixing ratio. Besides, the conversion of the inlet gases and the selectivities of the reaction products are calculated. Syngas, higher hydrocarbons, and higher oxygenates are typically found to be important reaction products. Furthermore, the main underlying reaction pathways for the formation of syngas, methanol, formaldehyde, and other higher oxygenates are determined.



1. INTRODUCTION

Methane is currently mainly being used for home and industrial heating and for the generation of electrical power. However, it is a greatly underutilized resource for the production of chemicals and liquid fuels, mainly because it is one of the most stable molecules.¹ The direct synthesis of hydrocarbons starting from methane is not yet feasible, and the conventional indirect methods for partial and total oxidation of methane are characterized by poor yields and require large amounts of energy.² The utilization of natural gas as a chemical resource is currently limited to the production of synthesis gas (i.e., syngas: H₂ + CO) by steam reforming, which is a highly energy-intensive process.³ Therefore, the development of a process for the direct synthesis of higher hydrocarbons and oxygenates from methane in an energy-efficient way toward economy and environment would offer significant benefits.

The major difficulty for the direct conversion of methane exists in breaking the stable C–H bond. As mentioned above, the conventional methods, which make use of a high temperature and a noble catalyst, require large amounts of energy and are lacking selectivity.³ Atmospheric pressure nonthermal low-temperature plasmas can offer here a distinct advantage, because they enable in a unique way gas-phase reactions at ambient conditions. A range of different plasma activation mechanisms cause vibrational and electronic excitation, as well as ionization and dissociation of species, and in this way, gas conversion processes are induced. One example of such nonthermal plasma is the dielectric barrier discharge (DBD), which can be operated in a pressure range of 0.1–10 bar, while remaining at ambient temperature.

A DBD is generated between two electrodes of which at least one is covered with a dielectric material. The gap between the two electrodes is typically a few millimeters. An ac voltage with an amplitude of 1–100 kV and a frequency ranging from a few Hz to MHz are usually applied to this kind of discharges. Detailed information on the history and the characteristics of a DBD can be found in the literature.^{4–9}

DBDs can be used in a wide variety of applications.^{9–14} Nowadays, a lot of research is carried out on the use of a DBD for the conversion of CH₄ in the presence of a coreactant to higher hydrocarbons, oxygenates, and syngas. This coreactant has an important influence on the selectivities of the desired end products. Coreactants reported in the literature for the conversion of methane are, among others,^{15–19} oxygen,^{2,20–43} carbon dioxide,^{3,12,22,44–82} hydrogen,^{25,83,84} steam,^{78,81,85} and nitrogen.⁸⁶ When focusing on the formation of syngas and oxygenates, most research is performed on the partial oxidation with oxygen^{2,20,21,23–43} and on dry reforming (CO₂ reforming).^{3,12,44–77,79,80,82}

Of course, oxygen is very effective for low-temperature plasma activation of methane. However, a possible drawback is an excessive oxidation, resulting in the formation of CO₂ and a wide variety of oxygenates. Therefore, the use of CO₂ as a milder oxidant can sometimes be more preferable depending on the desired end product(s). Moreover, with CO₂ as a coreactant, the two most important greenhouse gases are converted in the process. Current interests in CO₂ utilization

Received: July 7, 2015

Revised: September 9, 2015

Published: September 10, 2015

include hydrogenation of CO₂ and the reforming of CH₄ by CO₂. However, application of the former is limited because of the high cost of hydrogen.⁴⁵

Experimental results on the conversion in CH₄/O₂^{2,20,21,23–43} and CH₄/CO₂^{3,12,44–77,79,80,82} plasmas show that the typical end products are C_xH_y, H₂, and CO, and, to a lower extent, also CH₃OH, CH₂O, and other higher oxygenates (acids, alcohols, aldehydes, esters, ketones, ...). In most papers, the focus is largely on the formation of C_xH_y and syngas. Only a few papers^{3,22–27,31,32,35,39–43,46,56,58,68,72,76} explicitly focus on the formation of CH₃OH, CH₂O, and other higher oxygenates.

In order to develop a sustainable industrial process, the yields and selectivities of the desired end products and the energy efficiency of the process should be optimized. Therefore, a better insight into the complicated underlying plasma chemistry acting in the conversion process would be of great value. Fluid modeling can offer here the necessary information.

Modeling results on the plasma chemistry in CH₄/O₂ and CH₄/CO₂ mixtures reported in the literature mostly originate from zero-dimensional simulations, largely based on specific empirical input, which is only valid for the experimental setup under study.^{18,21,34,41–44,57,76,87–90} Zhou et al. used a semi-empirical kinetic model to simulate the accumulated chemical action of many microdischarges in CH₄/O₂²¹ and CH₄/CO₂⁴⁴ gas mixtures. Besides the densities of the inlet gases and main products, the pathways for formation of methanol in CH₄/O₂ and syngas in CH₄/CO₂ were briefly discussed. Nair et al.,³⁴ Matin et al.,⁸⁹ Ağiral et al.,⁴² Goujard et al.,⁴¹ and Zhou et al.⁴³ used a semiempirical kinetic model to simulate the conversion in a CH₄/O₂ nonthermal plasma. Ağiral et al.⁴² briefly discussed the mechanisms of the gas-to-liquid process governing the formation of oxygenates. Goujard et al.⁴¹ performed calculations for two different temperatures and discussed the main underlying pathways for the formation of higher oxygenates at these temperatures. Kraus et al.¹⁸ and Luche et al.⁸⁸ used a semiempirical kinetic model to simulate the conversion in a CH₄/CO₂ and in a CH₄/air nonthermal plasma, respectively. Goujard et al. applied a simplified global kinetic model to study the helium dilution effect on CO₂ reforming of CH₄ in a DBD.⁷⁶ Snoeckx et al. performed a computational study ranging from the nanoseconds to seconds time scale for the conversion of CH₄ and CO₂ into value-added chemicals in a DBD.⁹⁰ A zero-dimensional chemical kinetics model was applied to study the plasma chemistry in a 1:1 CH₄/CO₂ gas mixture. The calculations were first performed for one microdischarge pulse and its afterglow. Subsequently, long time scale simulations were carried out, corresponding to real residence times in the plasma, assuming a large number of consecutive microdischarge pulses. The conversion of CH₄ and CO₂ as well as the selectivity of the formed products were calculated and compared to experiments for a range of different powers and gas flows. In a follow-up paper, the authors applied this model to a wide range of conditions, including gas mixing ratio, gas residence time, power, and frequency, to investigate which conditions give rise to the best conversion and energy efficiency.⁹¹ Machrafi et al. performed calculations for a 1:1 CH₄/CO₂ gas mixture⁷³ by means of a so-called 3D “Incompressible Navier–Stokes” model with a strongly reduced kinetic mechanism, in order to determine the velocity fields. This model was combined with a convection–diffusion model in order to study the behavior of the inlet gases. Qualitative densities were shown as it was not possible to have a huge

kinetic precision using a 3D model. Wang et al. conducted a density functional theory (DFT) study to investigate the reaction mechanisms for the synthesis of oxygenates and higher hydrocarbons from CH₄ and CO₂ using cold plasmas.⁹² The main dissociation routes of the reactants were analyzed, and the formation of various products including syngas, higher hydrocarbons, and oxygenates was discussed. Istadi et al. developed a hybrid artificial neural network-genetic algorithm to simulate and optimize a catalytic–DBD plasma reactor in a CH₄/CO₂ gas mixture.⁹³ The effects of the CH₄/CO₂ feed ratio, total feed flow rate, discharge voltage, and reactor wall temperature on the conversion of the inlet gases and the selectivities of the main products were investigated.

In the present paper, we also present a modeling study for the conversion of CH₄ in the presence of O₂ or CO₂ into higher oxygenates and syngas. However, we make use of a 1D fluid model. This allows us to calculate also the fluxes toward the reactor walls and to take into account surface sticking and secondary electron emission, without losing any kinetic information. A drawback of this modeling approach is, however, that we do not take into account the filamentary behavior of a DBD, in contrast to some 0D model approximations,⁹⁰ as we assume a uniform discharge plasma.

In order to achieve this goal, we first developed a 1D fluid model to describe in detail the plasma chemistry in an atmospheric pressure DBD in pure CH₄.⁹⁴ In the present paper, this model is extended to describe the plasma chemistry in CH₄/O₂ and CH₄/CO₂ gas mixtures.

Unlike in most of the above-cited papers, we focus in detail on the main underlying pathways governing the conversion to higher oxygenates, and moreover, we make a comparison of those pathways between a mixture with O₂ and a mixture with CO₂.

The goal of our work is to determine whether these gas conversion processes in a DBD may occur in an energy-efficient way and thus whether a process can be developed that is competitive with currently existing or emerging technologies. In order to optimize such a process to become competitive, it is indeed essential to understand the underlying plasma chemistry. This is of great interest when a catalyst will be inserted in the plasma, which is the final goal of our work, to improve the selectivity of the conversion process and to obtain a higher yield for one or more of the reaction products. Indeed, it is thus essential to know whether a heterogeneous catalyst would act on one or more of the underlying gas-phase reactions.

We present here the most important results on the partial oxidation and the dry reforming of CH₄ into syngas, higher oxygenates, and higher hydrocarbons. First, the spatially averaged electron and radical densities as a function of time will be illustrated. Furthermore, the densities of the reaction products for a range of different initial gas mixing ratios, as well as the conversion of the inlet gases, will be discussed. Finally, the main underlying reaction pathways for the formation of syngas, methanol, and formaldehyde, which appear to be the main oxygenates produced, will be pointed out.

2. DESCRIPTION OF THE MODEL

Similar to our previous study on the conversion of pure CH₄ in a DBD, again, the one-dimensional fluid model, called Plasimo's MD2D,^{95,96} is applied. This fluid model consists of a set of coupled partial differential equations which are derived from the Boltzmann equation. More specifically, particle continuity

equations and drift–diffusion equations for the various species, as well as an electron energy balance equation, are solved. These equations are coupled to the Poisson equation, which yields the electric field. This set of coupled equations is solved iteratively in time and in space until convergence is reached. A more detailed description of the physics used in the model and of the numerical methods that are applied is reported by Hagelaar⁹⁷ and by Brok et al.⁹⁸ Detailed information about our specific use of the model and the applied boundary conditions can be found in De Bie et al.⁹⁴

The chemistry in a CH₄/O₂ and CH₄/CO₂ gas mixture is described by 75 species (electrons, molecules, ions, and radicals). As mentioned above, the previous model for pure CH₄ is extended. O₂ and CO₂ are included as extra feed gases. Furthermore, CO, H₂O, CH₂O, CH₃OH, and some other higher oxygenates are considered in the model, as they might be formed in the plasma. Similar to the model for pure CH₄, the radical and ionic species corresponding to the formation products of dissociation, ionization, and attachment reactions of these molecules are also taken into account. Although some vibrational and electronic excitation reactions are included in the model, vibrationally and electronically excited species are not taken into account separately in order to limit the number of species and reactions. Also, rotationally excited species are not taken into account in the model. Indeed, the electron energy required for rotational excitations is negligible compared with this for vibrational excitations.^{99,100} Table 1 presents an

Table 1. Overview of the Species Included in the Model, Besides the Electrons

molecules	CH ₄ , C ₂ H ₆ , C ₂ H ₄ , C ₂ H ₂ , C ₂ , C ₃ H ₈ , C ₃ H ₆ , C ₄ H ₂ , H ₂ , O ₃ , O ₂ , CO ₂ , CO, H ₂ O, H ₂ O ₂ , CH ₂ O, CH ₃ OH, C ₂ H ₅ OH, CH ₃ CHO, CH ₂ CO, CH ₃ OOH, C ₂ H ₅ OOH
ions	CH ₃ ⁺ , CH ₄ ⁺ , CH ₅ ⁺ , CH ₂ ⁺ , CH ⁺ , C ⁺ , C ₂ H ₆ ⁺ , C ₂ H ₅ ⁺ , C ₂ H ₄ ⁺ , C ₂ H ₃ ⁺ , C ₂ H ₂ ⁺ , C ₂ H ⁺ , C ₂ ⁺ , H ₃ ⁺ , H ₂ ⁺ , H ⁺ , O ₄ ⁺ , O ₃ ⁺ , O ₂ ⁺ , O ⁺ , O ₄ ⁻ , O ₃ ⁻ , O ₂ ⁻ , O ⁻ , CO ₂ ⁺ , CO ⁺ , H ₃ O ⁺ , H ₂ O ⁺ , OH ⁺ , H ⁺ , OH ⁻
radicals	CH ₃ , CH ₂ , CH, C, C ₂ H ₃ , C ₂ H ₃ , C ₂ H, C ₃ H ₇ , C ₃ H ₅ , H, O, OH, HO ₂ , CHO, CH ₂ OH, CH ₃ O, C ₂ H ₅ O, C ₂ HO, CH ₃ CO, CH ₂ CHO, CH ₃ O ₂ , C ₂ H ₅ O ₂

overview of the different species taken into account in the model. Detailed information on the transport coefficients and wall interaction coefficients used can be found in De Bie et al.⁹⁴

The 75 species can interact with each other through a large number of reactions. 1019 gas-phase reactions, including 157 electron–neutral, 48 electron–ion, 476 neutral–neutral, and 338 ion–ion or ion–neutral reactions, are considered. An overview of the reactions is given in the Supporting Information.

The rates of the different reactions are calculated from the densities of the colliding species and the corresponding reaction rate coefficients. The electron–neutral and electron–ion reactions are treated by energy-dependent reaction rate coefficients. The rate coefficients of the electron–neutral reactions are obtained from look-up tables calculated with the Boltzmann solver Bolsig+,¹⁰¹ based on the energy-dependent collision cross sections for these reactions. The references for the cross sections can also be found in Table S.1 of the Supporting Information. The look-up tables for the electron–ion dissociative recombination reactions are built using the functions in combination with the branching ratios for the different channels, of which a detailed overview is given in Table S.2 of the Supporting Information. The neutral–neutral and ion–neutral reactions are defined in the model with a

constant reaction rate coefficient at a pressure and temperature of 1 atm and 300 K, respectively. These rate coefficients and their corresponding references are summarized in Tables S.3 and S.4 of the Supporting Information, respectively.

3. RESULTS AND DISCUSSION

The model is applied to a cylindrical DBD reactor, which consists of two coaxial electrodes. The inner electrode is grounded and has an outer diameter of 22 mm. The outer electrode is powered and has a diameter of 29.3 mm, and it is wrapped over a dielectric tube made of alumina. The alumina tube has an inner diameter of 26 mm and a wall thickness of 1.6 mm, resulting in a discharge gap of 2 mm between both cylinders. The length of the reactor segment under study is 1.5 mm. The initial gas temperature and pressure are assumed to be 300 K and 1 atm, respectively. The gas temperature is kept constant in time and in space. Thus, it should be realized that the thermochemistry of the reactions is not considered in this study. Indeed, the setup under consideration is cooled to keep the temperature constant.¹⁰² The initial gas density is calculated from the ideal gas law and corresponds to $2.446 \times 10^{25} \text{ m}^{-3}$, but the total density of gas molecules, and thus the pressure, will slightly change during the reactions, due to the production of new molecules. More information about the reactor setup can be found in De Bie et al.⁹⁴

The calculations are carried out for a gas residence time up to 20 s, at a fixed applied voltage of 5 kV and a frequency of 10 kHz. The CH₄/CO₂ molar ratio is varied in the range of 5–80% CO₂, while the CH₄/O₂ molar ratio is varied from 10% to 30% O₂. The CH₄/CO₂ molar ratio can be varied in a much wider range than the CH₄/O₂ molar ratio, because the latter approaches the upper flammability or explosion limit when the mole fraction of CH₄ in pure O₂ reaches 61 mol %.¹⁰³

First, the spatially averaged electron and radical densities as a function of time will be shown for both gas mixtures, and the densities of the formed end products as a function of the initial gas mixing ratio will be discussed (section 3.1). Subsequently, in section 3.2, the conversion of the inlet gases will be presented as a function of time and as a function of the initial gas mixing ratio, and the yields and selectivities of the main products will be illustrated. Finally, in section 3.3, the dominant reaction pathways for the formation of syngas, methanol, and formaldehyde will be pointed out by means of schematic overviews, and a comparison will be made between a 70/30 CH₄/CO₂ and a 70/30 CH₄/O₂ gas mixture.

3.1. Densities of the Plasma Species. Figure 1 illustrates the periodic behavior as a function of time of the spatially averaged electron density for a 70/30 (a) and 90/10 (b) CH₄/O₂ gas mixture and for a 70/30 (c) and 90/10 (d) CH₄/CO₂ gas mixture, on a logarithmic scale, for four periods of the applied voltage. The applied voltage as a function of time is also plotted, for the sake of clarity. In the 70/30 CH₄/O₂ mixture, breakdown in the gas appears once each period following the applied voltage, while, in the 90/10 CH₄/O₂ mixture and the 70/30 CH₄/CO₂ mixture, a breakdown appears each half period, and in the 90/10 CH₄/CO₂ mixture, even more breakdowns occur (see below). The electron density behavior is different for the positive and the negative polarity of the applied voltage, which is due to the dissimilarity in surface dimensions and properties of the inner and outer electrodes (i.e., only the outer electrode is covered by a dielectric), as was also discussed in De Bie et al.⁹⁴

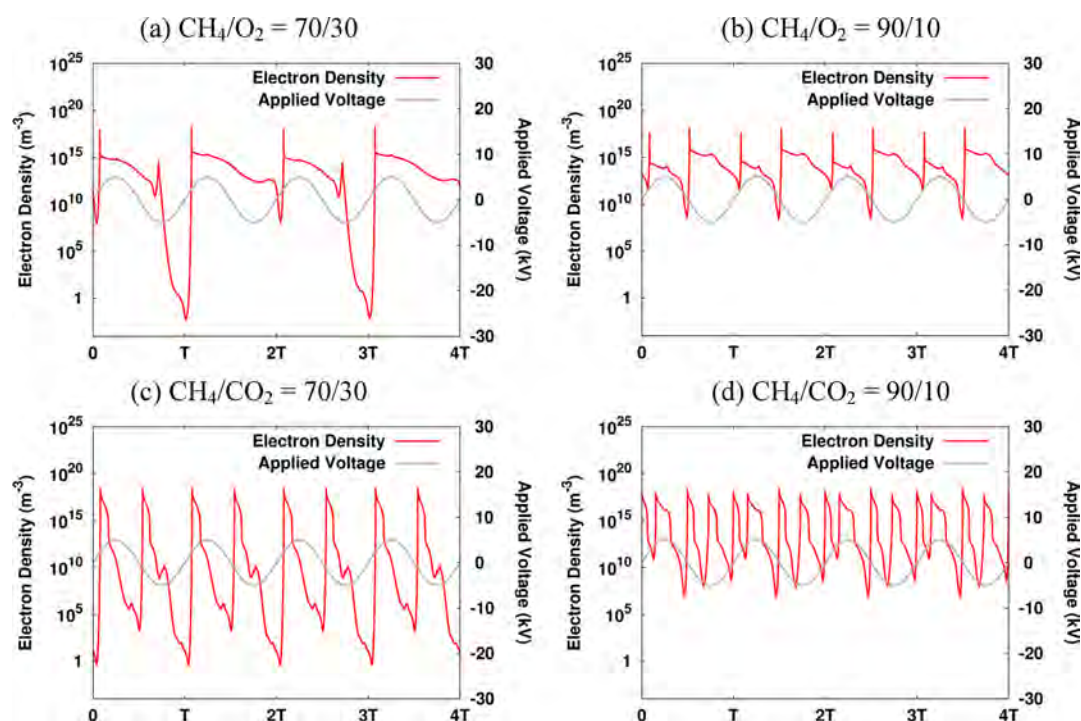


Figure 1. Spatially averaged electron density on a logarithmic scale for a 70/30 (a) and 90/10 (b) CH_4/O_2 gas mixture and for a 70/30 (c) and 90/10 (d) CH_4/CO_2 gas mixture, as a function of time, for four periods of the applied voltage. The applied sinusoidal voltage is also presented, for the sake of clarity.

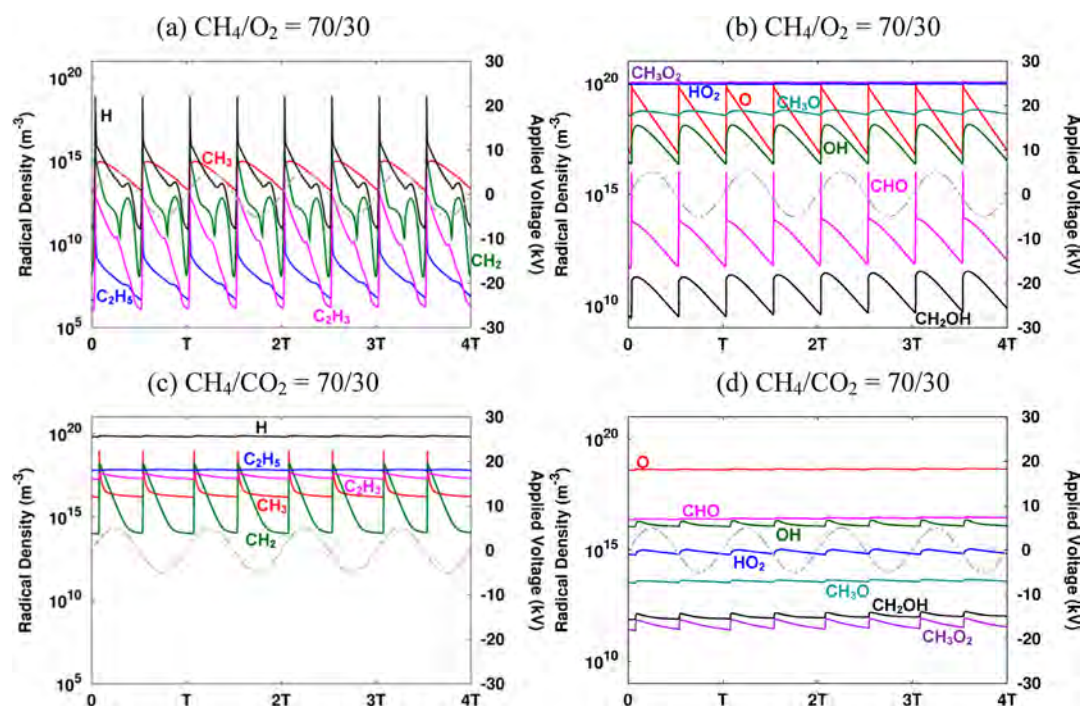


Figure 2. Spatially averaged radical densities (left axis) as a function of time for a 70/30 CH_4/O_2 (a, b) gas mixture and for a 70/30 CH_4/CO_2 (c, d) gas mixture, as well as the applied sinusoidal voltage (gray, right axis) for four periods of the applied voltage.

As mentioned above, in the mixtures with CO_2 , twice as many breakdowns appear, compared to the corresponding mixtures with O_2 . The panels (a \leftrightarrow c, b \leftrightarrow d) (Figure 1) also illustrate the different periodical behavior. Furthermore, the number of breakdowns is also twice as large for the mixtures with 90% CH_4 (b and d) compared to the corresponding mixtures with 70% CH_4 (a and c). The same behavior was also

observed for the current profiles and the charging of the electrodes and can be attributed to the different degree of electronegativity of the various gas mixtures and mixing ratios (see below).

It is also clear from the panels that, for the mixtures with 90% CH_4 (b and d), the minimum electron density is much higher than for the mixtures with 70% CH_4 (a and c) (Figure 1).

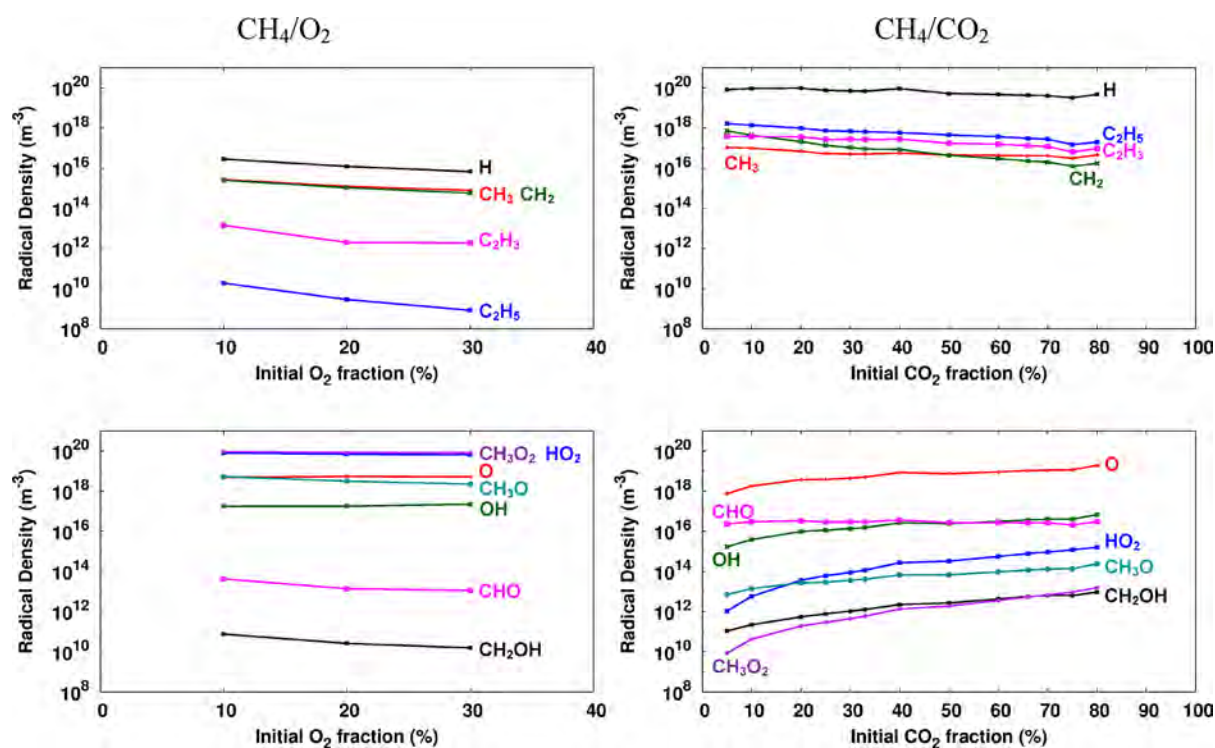


Figure 3. Spatially and time-averaged radical densities as a function of the initial gas mixing ratio for the CH_4/O_2 (left panel) and CH_4/CO_2 (right panel) gas mixtures.

Nevertheless, the overall spatially and time-averaged electron density is almost the same for either 90% or 70% CH_4 , and amounts to ca. 10^{15} m^{-3} for the CH_4/O_2 mixture and to ca. 10^{16} m^{-3} for the CH_4/CO_2 mixture. This is 1 and 2 orders of magnitude lower than the calculated value of 10^{17} m^{-3} for a pure CH_4 plasma,⁹⁴ and the reason for this is given below.

The overall spatially and time-averaged mean electron energy in the CH_4/O_2 and CH_4/CO_2 gas mixtures was calculated to be about 1.6 eV and about 2.1 eV, respectively, compared to about 2 eV in pure CH_4 .⁹⁴ These differences in electron density and mean electron energy between CH_4/O_2 and CH_4/CO_2 can be attributed to the fact that CH_4/O_2 gives rise to an electronegative plasma in contrast to CH_4/CO_2 . Indeed, the (positive and negative) ion density is 3 orders of magnitude higher than the electron density in CH_4/O_2 , while, in CH_4/CO_2 , the electron density is in the same order of magnitude as the positive ion density and 1 order of magnitude higher than the negative ion density. This can be explained because, in CH_4/O_2 , the electrons are more easily trapped by attachment reactions with O_2 , and moreover, the higher energy electrons are more frequently consumed in ionization and dissociation reactions as the threshold energies for these reactions are much lower in CH_4/O_2 ^{104,105} than in CH_4/CO_2 .¹⁰⁶ Thus, the CH_4/O_2 plasma is most electronegative, containing the highest negative ion density, and this explains the lower (spatially and time-averaged) electron density than in the CH_4/CO_2 plasma (which still contains some negative ions), and especially compared to the pure CH_4 plasma (which does not contain negative ions).

The number densities of the radicals and ions, produced by collisions of the electrons with the gas molecules, exhibit the same periodic behavior as the electron density, as is illustrated in Figure 2 for the radicals, for a 70/30 CH_4/O_2 (a, b) gas mixture and a 70/30 CH_4/CO_2 (c, d) gas mixture. However,

this periodic trend is superimposed on a rising or declining trend, acting over a longer time scale until a periodic steady state is reached.

It is clear from Figure 2 that the densities of some radicals, such as O, OH, CHO, CH_2OH , C_2H_3 , C_2H_5 , and H, in the CH_4/O_2 gas mixture, and CH_3 and CH_2 in both gas mixtures, vary over several orders of magnitude throughout a period. This is because their formation or loss (e.g., H radicals are consumed in reactions with O_2) is strongly dependent on electron impact dissociation of one of the inlet gases. On the other hand, the densities of radicals which are not directly formed by electron impact dissociation of one of the inlet gases, such as C_2H_5 , C_2H_3 , H, O, OH, CHO, and CH_2OH in the CH_4/CO_2 gas mixture, and HO_2 , CH_3O , and CH_3O_2 in both gas mixtures, vary by less than 1 order of magnitude throughout a period. The overall spatially and time-averaged radical densities vary from about 10^8 m^{-3} for the less abundant radicals, to about 10^{19} m^{-3} for the most abundant radicals. The most abundant radicals in the CH_4/O_2 gas mixture are O, OH, HO_2 , CH_3O , and CH_3O_2 , while H, O, CH_3 , CH_2 , C_2H_3 , and C_2H_5 are mostly abundant in the CH_4/CO_2 gas mixture (see also below). This will determine the different reaction pathways for the formation of the oxygenates in the CH_4/O_2 and CH_4/CO_2 gas mixtures, as will be elaborated in section 3.3, below.

Figure 3 shows the spatially and time-averaged radical densities as a function of the initial gas mixing ratio in both the CH_4/O_2 and the CH_4/CO_2 gas mixtures. It is clear that the mixtures with CO_2 , at an identical initial fraction of CH_4 , yield higher densities of C_xH_y , H, CHO, and CH_2OH radicals than the mixtures with O_2 , while the densities of O, OH, HO_2 , CH_3O , and CH_3O_2 are higher in the mixtures with O_2 than in the mixtures with CO_2 . This can be explained because the net formation of C_xH_y directly or indirectly from CH_4 is higher in the mixtures with CO_2 . Furthermore, the formed H, CHO, and

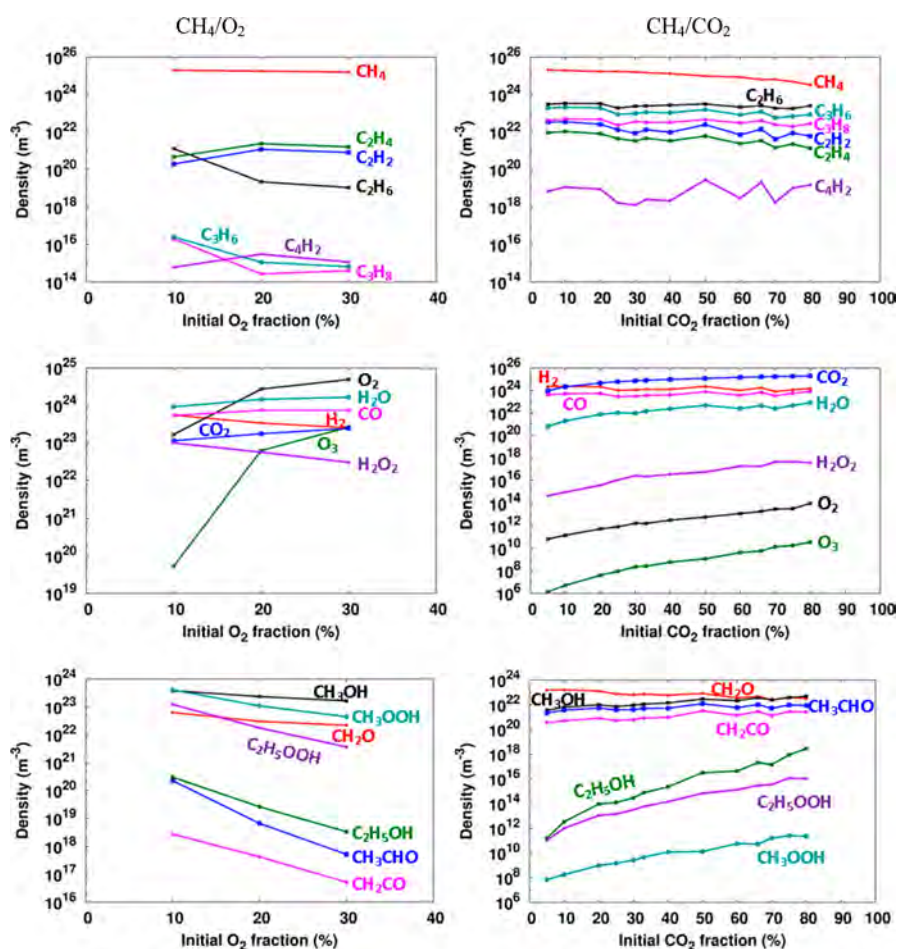


Figure 4. Spatially averaged molecule densities as a function of the initial gas mixing ratio, after a residence time of 5 s, for the CH₄/O₂ (left panel) and CH₄/CO₂ (right panel) gas mixtures.

CH₂OH radicals immediately react with O₂ into HO₂, CO, and CH₂O, respectively, and therefore, the net formation of H, CHO, and CH₂OH is higher in the mixtures with CO₂. Likewise, the O, OH, HO₂, CH₃O, and CH₃O₂ radicals are directly or indirectly formed from O₂ (see section 3.3, below), which explains their higher density in the CH₄/O₂ mixtures. Upon rising initial fraction of CO₂ between 5% and 80%, the densities of the C_xH_y radicals and of the H atoms drop by half an order to 1 order of magnitude, due to the fact that these radicals are directly or indirectly formed out of CH₄. A similar trend is observed upon rising fraction of O₂. On the other hand, the densities of O, OH, and other O-containing radicals increase by half an order to several orders of magnitude upon rising fraction of CO₂ in the gas mixture, which can be explained by the fact that these radicals are directly or indirectly formed out of CO₂. For the same reason, the densities of the O and OH radicals increase a bit upon rising fraction of O₂ in the gas mixture, while the other O-containing radicals decrease by half an order to several orders of magnitude. The latter can be explained by the fact that a higher inlet fraction of O₂ leads toward full oxidation of CH₄ (see also Figure 4, below).

The ion densities also exhibit a similar periodic behavior as the electrons, which is logical, as they are mostly formed by electron impact ionization or by (dissociative) attachment from the inlet gases, for the positive and negative ions, respectively. The most abundant ions in the CH₄/O₂ gas mixtures are CH₅⁺, C₂H₅⁺, O₄⁺, H₃O⁺, O₂⁻, O₄⁻, and OH⁻, while CH₅⁺, C₂H₅⁺,

and OH⁻ are the most abundant ions in the CH₄/CO₂ gas mixtures. Their spatially and time-averaged densities are in the order of 10¹⁷ m⁻³ and 10¹⁶ m⁻³ for the CH₄/O₂ and CH₄/CO₂ gas mixtures, respectively. This is typically 2 or 3 orders of magnitude lower than the spatially and time-averaged densities of the most abundant radicals in both gas mixtures, indicating that the ions play a minor role in the plasma chemistry (see section 3.3, below). Therefore, we do not go in further detail on the ion densities.

The molecules do not exhibit such a periodic behavior as the electrons, as they are not directly correlated with the electron density and electron energy, because they are typically formed by recombination of the radicals (see section 3.3, below). The densities of the molecules formed from the inlet gases, i.e., H₂, CO, higher-order hydrocarbons, and oxygenates, exhibit a rising trend as a function of time, during each half period of the applied voltage, because their net production is higher than their net consumption. The inlet gases, on the other hand, have a higher net consumption, so they are characterized by a gradual decrease in their densities during each half period. It appears that the conversion is most pronounced in the first few seconds and that the densities of the molecules do not significantly change anymore for a longer residence time. Below, we present the densities as a function of time, but here, we first focus on the densities of the different end products as a function of the initial gas mixing ratio after a certain residence time.

Figure 4 illustrates the densities of the various molecules as a function of the initial gas mixing ratio, after a residence time of 5 s, for the CH₄/O₂ (left panel) and CH₄/CO₂ (right panel) gas mixtures. A residence time of 5 s corresponds to a gas flow rate of 0.2 L·min⁻¹ for the plasma reactor under study.⁹⁴ It is clear that the densities of the higher hydrocarbons (C_xH_y), as well as H₂, CH₂O (formaldehyde), CH₃CHO (acetaldehyde), and CH₂CO (ketene or ethenone), are higher in the mixtures with CO₂, while the densities of O₃, H₂O, H₂O₂ (hydrogen peroxide), CH₃OH (methanol), C₂H₅OH (ethanol), CH₃OOH (methyl hydroperoxide), and C₂H₅OOH (ethyl hydroperoxide) are higher in the mixtures with O₂. CO is formed at high density in both gas mixtures, and therefore, the H₂/CO ratio is higher than 1 in the mixtures with CO₂ and lower than 1 in the mixtures with O₂. Note that, in the gas mixtures with O₂ as a coreactant, also a significant amount of undesired CO₂ is formed.

These results are in good agreement with reported results in the literature on the formation of oxygenates in CH₄/O₂ and CH₄/CO₂ in discharges at similar conditions. Larkin et al.^{22,24–26} discussed the formation of CO, CO₂, CH₃OH, CH₂O, HCOOH (formic acid), and CH₃COOH (acetic acid) in CH₄/O₂ in a plasma reactor surrounded by a water cooling jacket to increase the formation of liquid oxygenates. They also showed that, in the presence of enough O₂, the selectivity of C_xH_y will remain low. Okumoto et al.^{23,27} made use of dilution gases to enhance the formation of oxygenates in CH₄/O₂ and reported the formation of C_xH_y, CO, CO₂, H₂, H₂O, CH₃OH, CH₂O, and CH₃CHO. Nozaki et al.,^{31,39,40} Goujard et al.,⁴¹ and Ağiral et al.⁴² carried out experiments for CH₄/O₂ gas mixtures in a microplasma reactor, which was immersed into a water bath maintained near room temperature to enhance the condensation of liquid components on the cooled reactor wall. Furthermore, they intermittently injected distilled water in addition to the inlet gases in order to wash out these liquid components and they collected all condensable components at the end of the reactor by a cold trap. They found that, if oxygen was totally consumed, so after a long residence time, or when the inlet oxygen fraction was excessively high, the main products were CO, CO₂, and H₂O. Besides also the formation of H₂, C_xH_y, HCOOH, H₂O₂, CH₃OOH, CH₃OH, and CH₂O were reported, and the concentration of CH₃OH was much higher than that of CH₂O without the cooling, which is in good agreement with our results. However, the selectivity of CH₂O and HCOOH drastically increased when cooling the reactor. Indarto et al.^{32,35} discussed the formation of H₂, CO, CO₂, H₂O, C_xH_y, and CH₃OH in CH₄/O₂ and found that a proper selection of catalyst can drastically enhance the yield and selectivity of CH₃OH. Our results are also in reasonable agreement with the results reported by Zhou et al.⁴³ comparing the use of a single and a double dielectric plasma reactor for the direct oxidation of CH₄ to H₂O₂ and oxygenates, where the double dielectric reactor favored the formation of these products.

The conversion of CH₄ in the presence of CO₂ is much less reported. Zou et al.³ discussed the formation of CO, H₂, C_xH_y, H₂O, CH₂O, CH₃OH, C₂H₅OH, HCOOH, CH₃COOH and other alcohols, acids, aldehydes, ketones, and esters in CH₄/CO₂ in the presence of starch. It was shown that the selectivity of C_xH_y was much higher than for the oxygenates, which is in good agreement with our results. Kozlov et al.,⁴⁶ Zhang et al.,⁵⁸ and Scarduelli et al.⁷² reported the formation of a variety of hydrocarbons and oxygenates in CH₄/CO₂. Li et al.⁵⁶ found

that CH₃COOH and C₂H₅OH were the major oxygenates among other alcohols and acids formed in CH₄/CO₂, but of course, their selectivities were much lower than those for C_xH_y and CO. Sentek et al.⁶⁸ discussed the formation of H₂, CO, C_xH_y, and alcohols in a CH₄/CO₂ plasma in the presence of a catalyst. Finally, Goujard et al.⁷⁶ studied the effect of helium dilution on the formation of CO, C_xH_y, CH₂O, and CH₃OH in CH₄/CO₂.

The flexible adaptation of the H₂/CO ratio in a DBD by altering the inlet gas mixing ratio is an advantage compared to classical processes, including steam reforming, partial oxidation, and CO₂ reforming, which typically produce syngas with H₂/CO molar ratios of >3, <2, and <1, respectively.^{44,49} The H₂/CO molar ratio from steam reforming (>3) is much higher than that required by the stoichiometry for many synthesis processes. A low H₂/CO molar ratio is desirable for many industrial synthesis processes, such as the Fischer–Tropsch synthesis or the synthesis of valuable oxygenated chemicals. Methanol can even be produced from syngas with a H₂/CO molar ratio as low as 0.5, when the system can simultaneously carry out methanol synthesis and the water-gas-shift reaction.^{44,49}

If the initial fraction of O₂ increases from 10% to 30%, the densities of C₂H₆, C₃H₆, C₃H₈, H₂, H₂O₂, CH₂O, CH₃OH, and CH₃OOH decrease up to 1 order of magnitude, and the densities of C₂H₅OH, CH₃CHO, CH₂CO, and C₂H₅OOH decrease even with several orders of magnitude. Meanwhile, the densities of C₂H₄, C₂H₂, C₄H₂, CO₂, CO, and H₂O increase up to 1 order of magnitude and the density of O₃ increases with several orders of magnitude, pointing toward full oxidation of CH₄. In other words, if higher oxygenates, such as CH₂O and CH₃OH, are the desired end products of the gas conversion of CH₄, it is appropriate to make use of CH₄/O₂ gas mixtures with a not too high fraction of O₂. These results are in reasonable agreement with the reported research on the effect of the initial gas mixing ratio in similar discharges in CH₄/O₂ by Larkin et al.,^{24,26} Okumoto et al.,²⁷ and Zhou et al.⁴³

Likewise, increasing the initial fraction of CO₂ from 5% to 80% results in a drop of the densities of C_xH_y, H₂, and CH₂O up to 1 order of magnitude, while the densities of CO, CH₃OH, CH₃CHO, and CH₂CO increase up to 1 order of magnitude and the densities of O₂, O₃, H₂O, H₂O₂, C₂H₅OH, CH₃OOH, and C₂H₅OOH increase even with several orders of magnitude. In other words, the ideal gas mixing ratio for CH₄/CO₂ gas mixtures depends on the desired higher oxygenate to be formed. Since the H₂ density drops and the CO density increases upon rising initial fractions of O₂ and CO₂, the H₂/CO molar ratio will significantly decrease, which is interesting, in view of the desired stoichiometry for industrial synthesis processes (cf. above). These results are again in reasonable agreement with literature studies on the effect of the initial gas mixing ratio in similar discharges in CH₄/CO₂ by Zou et al.,³ Li et al.,⁵⁶ and Zhang et al.⁵⁸

Note that the trends illustrated in Figure 4 correspond to a residence time of 5 s. However, the different molecules might have their maximum densities at a different residence time for the different gas mixtures studied, so the trends depicted in Figure 4 are not necessarily the same at other residence times. Besides, the gas composition in the CH₄/O₂ gas mixtures completely changes at the moment when O₂ is fully consumed, which happens after 5.6 and 15.2 s, in the case of 10% and 20% O₂, respectively (see Figure 6, below).

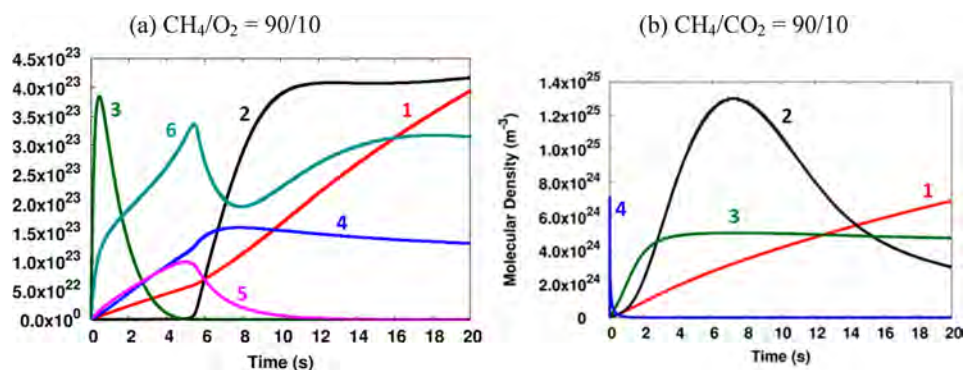


Figure 5. Spatially averaged molecule densities as a function of the residence time, for the 90/10 CH_4/O_2 gas mixture (a) and the 90/10 CH_4/CO_2 gas mixture (b). The labels of the curves characterize some specific molecules (see text). For panel (a): 1 = H_2 (density divided by 10), 2 = C_2H_6 , 3 = O_3 (density multiplied by 10), 4 = CO_2 , 5 = H_2O_2 , 6 = CH_2O (density multiplied by 5). For panel (b): 1 = H_2 , 2 = C_2H_4 (density multiplied by 1000), 3 = C_3H_8 (density multiplied by 100), 4 = O_2 (density multiplied by 10^{10}).

To make this more clear, we show in Figure 5 the characteristic density profiles as a function of the residence time, as we have observed for the different molecules, for a 90/10 CH_4/O_2 (a) and a 90/10 CH_4/CO_2 (b) gas mixture.

In the mixture with O_2 , we can distinguish six different density profiles:

1. H_2 and CO show a continuously rising trend.
2. The higher hydrocarbons (C_xH_y), ethanol ($\text{C}_2\text{H}_5\text{OH}$), and ketene (CH_2CO) have negligible values up to 5.6 s, followed by a strong increase up to an equilibrium value after 10 s.
3. O_3 exhibits a maximum within 1 s, and then reacts away within 3 s.
4. CO_2 , H_2O , and methanol (CH_3OH) show a steady increase to a maximum at around 6–8 s, followed by a very slow decrease.
5. Hydrogen peroxide (H_2O_2), methyl hydroperoxide (CH_3OOH), and ethyl hydroperoxide ($\text{C}_2\text{H}_5\text{OOH}$) go over a maximum at 4–6 s and then decrease rapidly.
6. Finally, formaldehyde (CH_2O) and acetaldehyde (CH_3CHO) also reach a maximum at 4–6 s, but after a fast drop, their density increases again after 8 s.

Except for the profile of O_3 (no. 3) (Figure 5), which has already reacted away after 4 s, the effect of O_2 being fully consumed after 5.6 s can be observed in the changes of the density profiles of all different molecules at this moment of time. Indeed, the densities of the higher hydrocarbons, for instance, start rising at that time, because, in the absence of O_2 , the CH_4 will mainly be converted into higher hydrocarbons, while the densities of the oxygenates typically show a (sharp) drop in time, when O_2 is fully depleted.

In the mixture with CO_2 , four different density profiles can be distinguished:

1. H_2 , CO , ethane (C_2H_6), and methanol (CH_3OH) exhibit a steady rise as a function of time.
2. Ethylene (C_2H_4), acetylene (C_2H_2), C_4H_2 , H_2O , formaldehyde (CH_2O), acetaldehyde (CH_3CHO), and ketene (CH_2CO) go over a maximum at around 6–8 s.
3. Propane (C_3H_8), propene (C_3H_6), and ethanol ($\text{C}_2\text{H}_5\text{OH}$) rise rapidly, but reach an equilibrium density after 2 s.
4. O_2 , O_3 , hydrogen peroxide (H_2O_2), methyl hydroperoxide (CH_3OOH), and ethyl hydroperoxide

($\text{C}_2\text{H}_5\text{OOH}$) reach a maximum within 5 ms, and then react rapidly away.

Thus, it is clear that the higher hydrocarbons and oxygenates (nos. 2 and 3) (Figure 5) can be formed at rather high density, but they react away again after a longer residence time toward H_2 and CO , respectively, which explains why H_2 and CO show a continuously rising trend. Besides H_2 and CO , also C_2H_6 and CH_3OH exhibit a steady rise (no. 1) as their formation is strongly connected to the dissociation products of CH_4 , in particular, the CH_3 and CH_2 radicals. Finally, O_2 , O_3 , and the different peroxides are only present at very low densities, and for a very short time, as they are formed as an intermediate in the direct or indirect formation of CO .

An identical behavior is observed for all of these species in the other gas mixing ratios of CH_4 with O_2 and CO_2 .

3.2. Conversion of CH_4 , O_2 , and CO_2 and Yields and Selectivities of the Main Reaction Products. Before showing the conversions, yields, and selectivities, we first want to make clear which definitions are used for the conversion X , the yields Y , and the selectivities S

$$X_{\text{CH}_4/\text{CO}_2/\text{O}_2} = \frac{n_{\text{CH}_4/\text{CO}_2/\text{O}_2, \text{converted}}}{n_{\text{CH}_4/\text{CO}_2/\text{O}_2, \text{feed}}} \times 100\% \quad (1)$$

$$Y_{\text{H}_2} = \frac{n_{\text{H}_2}}{2 \times n_{\text{CH}_4, \text{feed}}} \times 100\% \quad (2)$$

$$Y_{\text{C}_x\text{H}_y\text{O}_z} = \frac{x \times n_{\text{C}_x\text{H}_y\text{O}_z}}{n_{\text{CH}_4, \text{feed}}} \times 100\% \quad (\text{CH}_4/\text{O}_2) \quad (3)$$

$$Y_{\text{C}_x\text{H}_y\text{O}_z} = \frac{x \times n_{\text{C}_x\text{H}_y\text{O}_z}}{n_{\text{CH}_4, \text{feed}} + n_{\text{CO}_2, \text{feed}}} \times 100\% \quad (\text{CH}_4/\text{CO}_2) \quad (4)$$

$$Y_{\text{H}_2\text{O}} = \frac{n_{\text{H}_2\text{O}}}{2 \times (n_{\text{CH}_4, \text{feed}} + n_{\text{O}_2, \text{feed}})} \times 100\% \quad (\text{CH}_4/\text{O}_2) \quad (5)$$

$$Y_{\text{H}_2\text{O}} = \frac{n_{\text{H}_2\text{O}}}{2 \times (n_{\text{CH}_4, \text{feed}} + n_{\text{CO}_2, \text{feed}})} \times 100\% \quad (\text{CH}_4/\text{CO}_2) \quad (6)$$

$$S_{\text{H}_2} = \frac{n_{\text{H}_2}}{2 \times n_{\text{CH}_4, \text{converted}}} \times 100\% \quad (7)$$

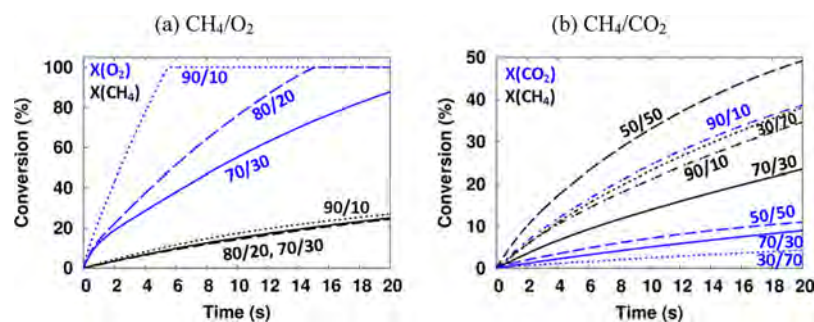


Figure 6. Conversion of CH_4 (black) and O_2 (a, blue) or CO_2 (b, blue) as a function of residence time.

$$S_{\text{C}_x\text{H}_y\text{O}_z} = \frac{x \times n_{\text{C}_x\text{H}_y\text{O}_z}}{n_{\text{CH}_4, \text{converted}}} \times 100\% \quad (\text{CH}_4/\text{O}_2) \quad (8)$$

$$S_{\text{C}_x\text{H}_y\text{O}_z} = \frac{x \times n_{\text{C}_x\text{H}_y\text{O}_z}}{n_{\text{CH}_4, \text{converted}} + n_{\text{CO}_2, \text{converted}}} \times 100\% \quad (\text{CH}_4/\text{CO}_2) \quad (9)$$

$$S_{\text{H}_2\text{O}} = \frac{n_{\text{H}_2\text{O}}}{2 \times (n_{\text{CH}_4, \text{converted}} + n_{\text{O}_2, \text{converted}})} \times 100\% \quad (\text{CH}_4/\text{O}_2) \quad (10)$$

$$S_{\text{H}_2\text{O}} = \frac{n_{\text{H}_2\text{O}}}{2 \times (n_{\text{CH}_4, \text{converted}} + n_{\text{CO}_2, \text{converted}})} \times 100\% \quad (\text{CH}_4/\text{CO}_2) \quad (11)$$

Note that the parameter x in these definitions denotes the stoichiometric balance coefficient, which corresponds also to the index in the compound name of $\text{C}_x\text{H}_y\text{O}_z$. Furthermore, note that the yield and selectivity of CO are calculated with $Y_{\text{C}_x\text{H}_y\text{O}_z}$ and $S_{\text{C}_x\text{H}_y\text{O}_z}$ respectively, with $y = 0$.

Figure 6 shows the conversion of CH_4 and O_2 (a) and of CH_4 and CO_2 (b) as a function of residence time for different gas mixing ratios. The conversion of CH_4 after 20 s is around 20% in all considered mixtures with O_2 , while, in pure CH_4 , a conversion of 40% was calculated after 20 s.⁹⁴ This is logical, because, in the CH_4/O_2 mixture, a considerable fraction of the energy is also consumed by O_2 . O_2 is indeed converted very quickly, and the time for full conversion depends on the initial fraction of O_2 . That is, full conversion is reached faster in the case of a lower O_2 initial fraction (see Figure 6a), which is logical.

In the CH_4/CO_2 gas mixture, the conversion of both CH_4 and CO_2 strongly depends on the initial gas mixing ratio. No clear trend can be observed from Figure 6b, because the initial gas mixing ratio strongly affects the discharge characteristics and, therefore, the conversion of the inlet gases. The effect of the initial gas mixing ratio on the conversion will be discussed below. Our calculations predict a maximum conversion of 68% for CH_4 and 55% for CO_2 after a residence time of 20 s in a 20/80 and a 95/5 CH_4/CO_2 gas mixture, respectively (not shown in Figure 6b). It is logical that a higher CH_4 conversion is reached at a lower initial CH_4 fraction in the gas mixture, and vice versa for CO_2 , because these conditions yield a higher coreactant concentration, which contributes to a more efficient conversion.

When comparing the conversion of CH_4 in both the CH_4/O_2 and the CH_4/CO_2 gas mixtures with the same gas mixing ratios, it is clear that, at a 70/30 gas mixing ratio, the CH_4 conversion is equal (i.e., around 20%) in both gas mixtures, while, at the 80/20 and 90/10 gas mixing ratios, the CH_4 conversion was

found to be slightly higher in the mixtures with CO_2 than in the mixtures with O_2 . This can be explained because the loss (by electron impact dissociation and ionization) of CH_4 is about a factor of 2 higher in CH_4/CO_2 than in CH_4/O_2 due to the fact that much more electrons are consumed by electron impact reactions with O_2 than with CO_2 (cf. the electronegative character, explained in section 3.1, above). However, the lower consumption of CH_4 in the CH_4/O_2 gas mixture is partially compensated by the increasing importance of the reaction with OH when the initial fraction of O_2 in the gas mixture increases. Furthermore, in the CH_4/CO_2 gas mixture, the production (or regeneration) of CH_4 is around 50% of the CH_4 consumption when the initial fraction of CO_2 is in the range of 10–30%, while, in the CH_4/O_2 mixture, the CH_4 production is decreasing with increasing O_2 initial fraction, from 30% of the CH_4 consumption in 90/10 CH_4/O_2 to 8% in 70/30 CH_4/O_2 (i.e., 1 order of magnitude lower than in 70/30 CH_4/CO_2). In other words, the much lower regeneration of CH_4 in the 70/30 CH_4/O_2 mixture than in the 70/30 CH_4/CO_2 mixture compensates enough for the lower consumption of CH_4 in the 70/30 CH_4/O_2 mixture than in the 70/30 CH_4/CO_2 mixture. This effect, together with the increasing importance of the reaction with OH radicals, results in an almost equal net conversion of CH_4 in both gas mixtures at a 70/30 gas mixing ratio (see more details in section 3.3 and Figure 8, below).

Figure 7 shows the conversion of CH_4 , O_2 , and CO_2 as a function of the initial gas mixing ratio, for both the CH_4/O_2

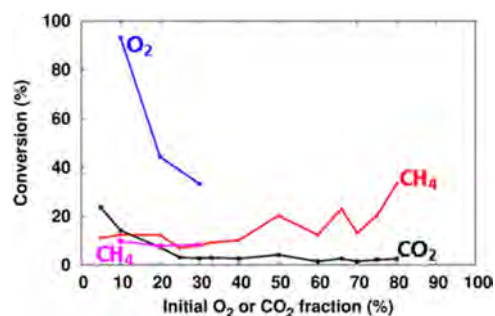


Figure 7. Conversion of CH_4 , O_2 , and CO_2 as a function of the initial O_2 or CO_2 fraction in the gas mixture, for a residence time of 5 s. The CH_4 conversion in the CH_4/CO_2 mixture is depicted in red, while the CH_4 conversion in the CH_4/O_2 mixture is presented in pink.

and the CH_4/CO_2 gas mixtures, after a residence time of 5 s. The CH_4 conversion is roughly independent from the initial O_2 or CO_2 fraction up to 30–40%, with a value of about 10%, but it increases for higher initial CO_2 fractions, especially above 70%. Indeed, at higher initial CO_2 fractions, the conversion of CH_4 rises due to the increasing importance of the reaction of

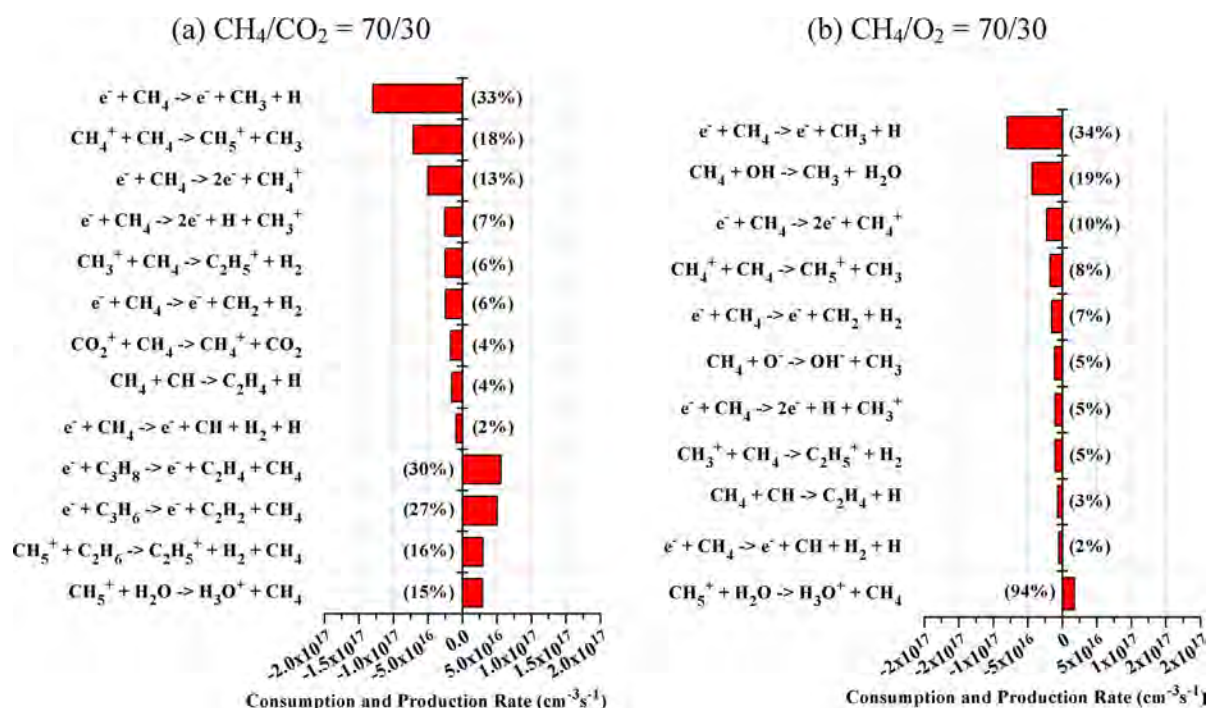


Figure 8. Time-averaged reaction rates of the dominant reaction pathways for the consumption and production of CH₄, for a 70/30 CH₄/CO₂ gas mixture (a) and a 70/30 CH₄/O₂ gas mixture (b). The consumption rates are defined as negative values (i.e., left-hand side of the figures), while the production rates are plotted as positive values (i.e., right-hand side of the figures). The relative contributions of these consumption and production processes to the overall consumption and production of CH₄ are also indicated.

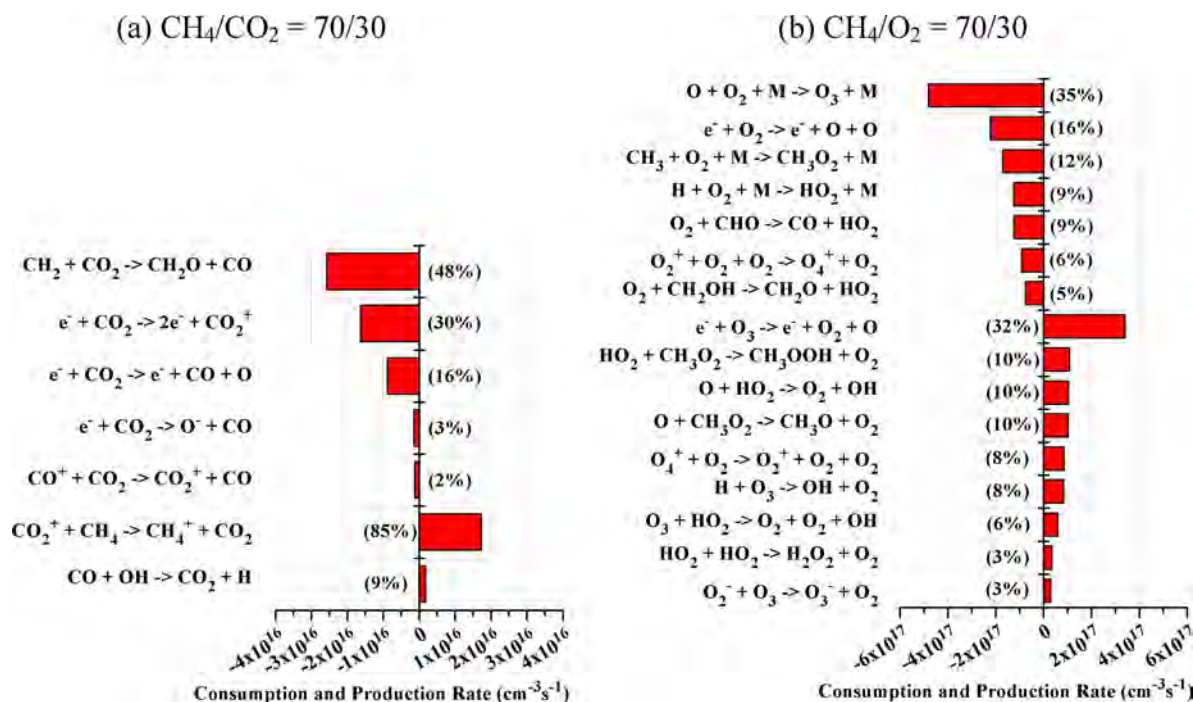


Figure 9. Time-averaged reaction rates of the dominant reaction pathways for the consumption and production of CO₂ for a 70/30 CH₄/CO₂ gas mixture (a) and for the consumption and production of O₂ for a 70/30 CH₄/O₂ gas mixture (b).

CH₄ with CO₂⁺, which becomes the most important channel for consumption of CH₄, while, at lower initial CO₂ fractions, electron impact dissociation of CH₄ is the most important loss channel (see also section 3.3 and Figure 8, below). For the same reason, the conversion of O₂ and CO₂ increases with decreasing initial O₂ or CO₂ fraction, because of the additional

loss reactions with CH₄ molecules (or CH₄-derived species). For instance, in the 70/30 CH₄/O₂ mixture, a three-body reaction with O radicals is the most important loss process for O₂, while, in the 90/10 CH₄/O₂ mixture, the most important loss processes for O₂ are three-body reactions with CH₃ or H radicals (see also section 3.3 and Figure 9, below). Likewise, in

Table 2. Overview of the Maximum Yields for Some Important End Products in Both the CH₄/O₂ and the CH₄/CO₂ Gas Mixtures, as Well as the Corresponding Gas Mixing Ratio and Residence Time at Which These Maximum Yields Are Obtained. The Corresponding Selectivities of These End Products Are Also Listed

		H ₂	CO	CH ₂ O	CH ₃ OH
CH ₄ /O ₂	yield (%)	9	10	0.3	4
	mixture	90/10	70/30	90/10 and 80/20	80/20
	residence time (s)	20	20	5.4 and 14.9	20
	selectivity (%)	33	39	3 and 2	15
CH ₄ /CO ₂	yield (%)	34	10	0.9	0.4
	mixture	20/80	20/80	90/10	25/75
	residence time (s)	20	20	10.3	20
	selectivity (%)	50	52	4	2

the CH₄/CO₂ mixtures with high initial CO₂ fractions, electron impact ionization of CO₂ is the most important loss channel, while, at lower initial CO₂ fractions, the reaction of CO₂ with CH₂ radicals is the most important loss channel for CO₂ (see again section 3.3 and Figure 9, below).

As was also clear from Figure 6, the O₂ conversion is much higher than the CO₂ conversion, which is only in the order of 20% at low CO₂ fractions, and even below 3% at higher CO₂ fractions. This is because the threshold energies for electron impact ionization and dissociation are much lower for O₂ than for CO₂. The CH₄ conversion is comparable to the CO₂ conversion at low CO₂ fractions, i.e., around 10%, but it rises to 35% at high CO₂ fractions. Finally, it is worth to mention that Figure 7 illustrates the conversion, relative to the amount of CH₄, CO₂, or O₂ present in the mixture. The absolute (or effective) conversion of CH₄ is of course higher at a higher initial CH₄ fraction, and vice versa for the absolute CO₂ and O₂ conversions, which is logical, as there is more of these gases initially present in the gas mixture.

Besides the conversion of CH₄, CO₂, and O₂, we are especially interested in the yields and selectivities of the formed value-added chemicals. Table 2 shows the maximum yields of H₂, CO, formaldehyde (CH₂O), and methanol (CH₃OH), as well as the gas mixtures and residence times for which these maximum values were obtained. Also, the corresponding selectivities are presented. Note that the sum of the selectivities does not have to be equal to 100%, because, in the CH₄/CO₂ mixture, the selectivities of CO, CH₂O, and CH₃OH are calculated with respect to both the CH₄ and the CO₂ conversions, while the H₂ selectivity is only calculated with respect to the CH₄ conversion. Similarly, in the case of the CH₄/O₂ mixture, the selectivities of CO, CH₂O, and CH₃OH are calculated with eq 8 above, while the H₂ selectivity is calculated with eq 7, resulting in a difference of a factor of 2.

Methanol is one of the most commonly used raw materials in the chemical industry. More than one-third of it is used in the production of formaldehyde; the rest is mainly utilized to produce acetic acid and gasoline octane improvers. Additionally, the direct use of methanol as fuel in internal combustion engines and fuel cells opens up the possibility of methanol-powered vehicles and consumer electronics.⁴² Formaldehyde is a common building block for the synthesis of more complex compounds, which are used in a wide range of products.

It is clear that syngas is the main product in both gas mixtures, but the H₂/CO molar ratio is somewhat different, as was also discussed in section 3.1, above. In the CH₄/O₂ mixture, the H₂ yield reaches a maximum at 10% O₂ fraction, while the CO yield reaches a maximum at 30% O₂ fraction, which is logical. In the CH₄/CO₂ mixture, the maximum H₂

and CO yields are both reached at 80% CO₂. For H₂, this can be explained because, although the absolute formation of H₂ is of course lower at a higher initial CO₂ fraction, its yield becomes higher as the latter is calculated with respect to the initial CH₄ density, which is obviously lower at a higher initial CO₂ fraction. For CO, electron impact dissociation of CO₂ is the most important production channel, and the highest density and yield of CO are found at the highest initial CO₂ fraction. Note that, at lower initial CO₂ fractions, the most important production channel of CO is the reaction of CH₂ radicals with CO₂, but this reaction does not lead to a higher CO density (see also section 3.3 and Figure 11, below). The H₂/CO molar ratio in the case of the 20/80 CH₄/CO₂ gas mixture is around 1.5, which is desirable for many industrial synthesis processes (cf. above). At higher CH₄/CO₂ gas mixing ratios, the H₂/CO molar ratio rises to about 5, because the H₂ density increases, while the CO density decreases upon higher CH₄ fraction in the mixture.

The maximum yields of CH₂O and CH₃OH are clearly lower than the maximum H₂ and CO yields. This is especially true in the CH₄/CO₂ mixtures, where both yields are below 1%. In this case, the highest CH₂O yield is obtained at 90% CH₄ fraction, while the highest CH₃OH yield is reached at 25% CH₄. In the CH₄/O₂ mixtures, the highest CH₂O yield is also below 1%, but the maximum CH₃OH yield reaches a value of 4%, which is not negligible. Nevertheless, a really selective production process toward CH₂O or CH₃OH seems not feasible in a DBD plasma, at least not at the conditions under study. We expect that, for this purpose, a catalyst will need to be integrated into the plasma region.

Finally, it is clear from Table 2 that the highest yields are not necessarily reached at the longest residence time. Indeed, the H₂, CO, and CH₃OH yields reach their maximum at 20 s residence time, pointing out that their densities are still rising as a function of time (cf. Figure 5, above), while the CH₂O yield clearly reaches its maximum at a shorter residence time (see also Figure 5, above), and the exact value depends on the gas mixture and gas mixing ratio, as it appears from Table 2. This indicates that, when the production of formaldehyde is targeted, the optimal residence time should be carefully selected.

Indeed, similar results were reported in the literature. Okumoto et al.²⁷ stated that CH₃OH and CH₂O are, in fact, intermediate products in the oxidation of CH₄ and are easily decomposed or converted to CO, CO₂, and H₂O. In other words, the formation of oxygenates is strongly dependent on the initial gas mixing ratio, the residence time, and a variety of other parameters. Okumoto et al. found that 15 vol % of O₂ showed optimum performance for the formation of CH₃OH

and CH₂O in CH₄/O₂.²⁷ Note that the authors made use of dilution gases to enhance the formation of oxygenates. Also, Zou et al.³ discussed the existence of an optimum feed composition to attain the maximum selectivity of the desired oxygenates. They obtained the highest total selectivity of oxygenates at a CH₄ concentration of 35 vol % in CH₄/CO₂ in the presence of starch with the highest selectivities of alcohols, such as CH₃OH, and acids when the CO₂ fraction in the feed increases to 74 vol %, and the highest selectivity of CH₂O at a higher CH₄ concentration of about 50 vol %. These findings are in reasonable agreement with our results.

3.3. Dominant Reaction Pathways. We will now discuss the dominant reaction pathways for the conversion of the inlet gases into syngas, higher-order hydrocarbons, and oxygenates for a 70/30 CH₄/CO₂ gas mixture and for a 70/30 CH₄/O₂ gas mixture.

(a). *Electron Impact Dissociation of CH₄, CO₂, and O₂: Initiating the Conversion Process.* As soon as the discharge is ignited, electron impact ionization and dissociation of the inlet gases occur, resulting in the creation of new species (electrons, ions, radicals), as discussed in section 3.1, above. The formation of new electrons and ions in the plasma enables sustaining the discharge, while the formation of radicals is important for the production of syngas, higher-order hydrocarbons, and oxygenates.

The dominant reactions for CH₄ consumption (and production) for a 70/30 CH₄/CO₂ gas mixture and a 70/30 CH₄/O₂ gas mixture are depicted in Figure 8a,b, respectively. Electron impact dissociations, yielding the formation of CH₃, CH₂, or CH radicals, are important channels for CH₄ consumption in both gas mixtures, with relative contributions of about 33, 6, and 2% in CH₄/CO₂ and 34, 7, and 2% in CH₄/O₂. In the 70/30 CH₄/O₂ gas mixture, the reaction with OH radicals, forming CH₃ radicals and H₂O, also contributes for about 19% to the loss of CH₄. This reaction is negligible in the CH₄/CO₂ mixture, due to the much lower OH radical density in that case (see Figure 2, above). Furthermore, also electron impact ionization and reactions with ions or radicals contribute to the loss of CH₄, accounting in total for about 20, 31, and 6%, respectively, in CH₄/CO₂ and for about 15, 21, and 22% (including the 19% of the reaction with OH), respectively, in CH₄/O₂.

It should be noted that electron impact vibrational excitation of CH₄ is also important, but this process is only considered in our model as an energy loss for the electrons, and not as a chemical loss process for CH₄, because the vibrationally excited species are not taken into account separately in our model.⁹⁴

The most important pathways for the production (or regeneration) of CH₄ in the mixture with CO₂ are based on electron impact dissociation of higher hydrocarbons, such as C₃H₈ and C₃H₆, while, in the mixture with O₂, these reactions appear negligible, and a charge transfer process of CH₅⁺ with H₂O is the most important production process.

Finally, it is clear from Figure 8 that the total production (or regeneration) rate of CH₄ in the 70/30 CH₄/CO₂ gas mixture is almost 1 order of magnitude higher than in the 70/30 CH₄/O₂ gas mixture, while the consumption rate in both gas mixtures is in the same order of magnitude. However, the total loss rate is still a factor of 2 higher than the total production rate in the CH₄/CO₂ mixture, and even a factor of 12 higher in the CH₄/O₂ mixture, resulting in a clear loss of CH₄.

At a higher initial CO₂ fraction, the reactions of CH₄ with CO₂⁺ and CH₄⁺ become the most important channels for the

consumption of CH₄ (see also section 3.2), accounting both for about 29% in 20/80 CH₄/CO₂, while the electron impact dissociation reaction yielding the formation of CH₃ only contributes for about 15% at these conditions. The most important pathway for the production (or regeneration) of CH₄ then becomes the charge transfer process of CH₅⁺ with H₂O, with a contribution of 32%. A decrease of the initial fraction of CO₂ results in an increase of the contributions of the electron impact dissociation reactions for the consumption of CH₄ and also an increase of the contributions of the electron impact dissociations of C₃H₈ and C₃H₆ for the regeneration of CH₄. A decrease of the initial fraction of O₂ to 10% results in a drastic decrease of the contribution of the reaction with OH radicals (3%). Electron impact dissociation yielding the formation of CH₃ remains the most important loss channel in this case, with a contribution of 42%. Meanwhile, the contribution of the charge transfer process of CH₅⁺ with H₂O, the most important production process of CH₄, decreases from 94% in 70/30 CH₄/O₂ to 38% in 90/10 CH₄/O₂, as electron impact dissociation of C₃H₈ and C₃H₆ becomes more important, like in the mixtures with CO₂.

The dominant reactions for CO₂ consumption (and production) for a 70/30 CH₄/CO₂ gas mixture and for O₂ consumption (and production) for a 70/30 CH₄/O₂ gas mixture are depicted in Figure 9a,b, respectively. The most important channel for consumption of CO₂ at this gas mixing ratio is the reaction with CH₂ radicals, contributing for about 48% to the CO₂ loss, followed by electron impact dissociation and ionization, which contribute for 16% and 30% to the total consumption of CO₂, respectively. At lower CO₂ fractions, the contribution of the first process will even increase to 77% for a 90/10 CH₄/CO₂ gas mixture. On the other hand, at higher CO₂ fractions in the gas mixture, the latter two processes will become gradually more important. For a 20/80 CH₄/CO₂ gas mixture, electron impact ionization and dissociation contribute for 52% and 27%, respectively, while the reaction with CH₂ radicals contributes for 9%. It is worth to mention that the reaction with CH₂ radicals is also the most important pathway for the production of CH₂O and CO in the 70/30 CH₄/CO₂ gas mixture (see below).

The most important channels for consumption of O₂ are three-body collisions with O, CH₃, or H radicals, with either CH₄, O₂, H₂O, or CO₂ as third body (denoted as M in Figure 9b), as well as electron impact dissociation of O₂ and a chemical reaction with CHO radicals. The three-body reaction with O radicals, forming O₃, is the most important loss process, with a contribution of 36%. However, almost all the O₃ will be decomposed back to O₂ by electron impact dissociation so that the net contribution of this reaction will be lower.

Electron impact dissociation of O₂ yields the formation of O radicals, while the reactions with CH₃, H, and CHO yield, among others, the formation of CH₃O₂ and HO₂. The O and HO₂ radicals will react further into OH (see below), which is an important species for the consumption of CH₄ (see above), while CH₃O₂ plays an important role in the formation of CH₃OH and CH₃OOH (see below). When the initial fraction of O₂ decreases to 10%, the three-body collisions with CH₃ and H radicals become more important for the consumption of O₂, with contributions of 29% and 25%, respectively. Meanwhile, the contribution of electron impact dissociation of O₂ decreases to 11% and the three-body collision with O radicals decreases drastically to 10%.

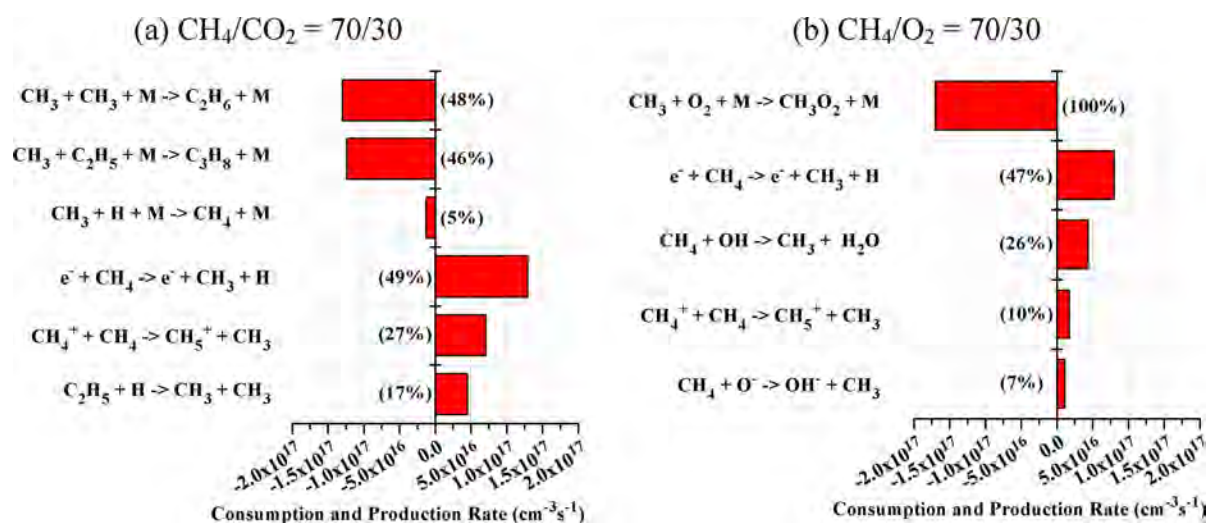


Figure 10. Time-averaged reaction rates of the dominant reaction pathways for the consumption and production of CH₃, for a 70/30 CH₄/CO₂ gas mixture (a) and for a 70/30 CH₄/O₂ gas mixture (b).

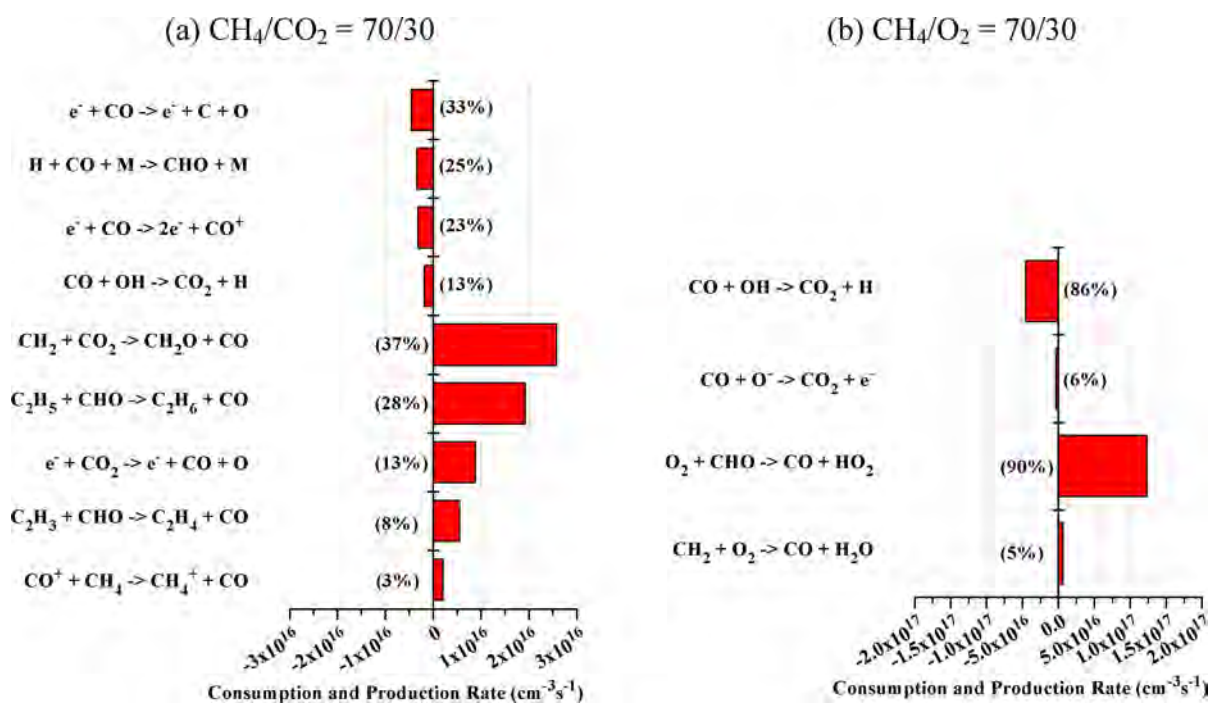


Figure 11. Time-averaged reaction rates of the dominant reaction pathways for the consumption and production of CO, for a 70/30 CH₄/CO₂ gas mixture (a) and a 70/30 CH₄/O₂ gas mixture (b).

The most important production mechanism for CO₂ in the CH₄/CO₂ gas mixtures is a charge transfer process between CO₂⁺ and CH₄, while electron impact dissociation of O₃ (see above) is the most important production process for O₂ in a 70/30 CH₄/O₂ gas mixture. As a result of the lower production of O₃ (see above) in a 90/10 CH₄/O₂ gas mixture, the reaction of HO₂ radicals with CH₃O₂ radicals toward CH₃OOH is the most important process for regeneration of O₂ in this mixture, with a contribution of 33%. However, the rates for regeneration of CO₂ and O₂ are again a factor of 2.6 and 1.3 lower than their corresponding loss rates so that there is a net consumption of CO₂ and O₂.

(b). *Recombination of CH₃ Radicals: The Formation of C_xH_y vs the Formation of CH₃O₂.* The most important species produced from CH₄ are the CH₃ radicals (see above). Figure

10a,b shows the dominant reactions for CH₃ consumption and production, again for a 70/30 CH₄/CO₂ gas mixture and a 70/30 CH₄/O₂ gas mixture, respectively. In the 70/30 CH₄/CO₂ mixture, the CH₃ radicals will mainly recombine toward higher hydrocarbons, such as C₂H₆ and C₃H₈, which contribute for 48% and 46% to the consumption of CH₃, respectively. On the other hand, in the 70/30 CH₄/O₂ gas mixture, these reactions are negligible compared to the three-body recombination reaction with O₂ molecules, forming CH₃O₂ radicals (see Figure 10b). This is in good agreement with Nozaki et al.⁴⁰ and Goujard et al.,⁴¹ who also discussed the importance of the formation of CH₃O₂ in the methane partial oxidation mechanism toward the formation of CH₃OH. Furthermore, this result explains the lower densities for the higher hydrocarbons in the gas mixtures with O₂ as coreactant (see

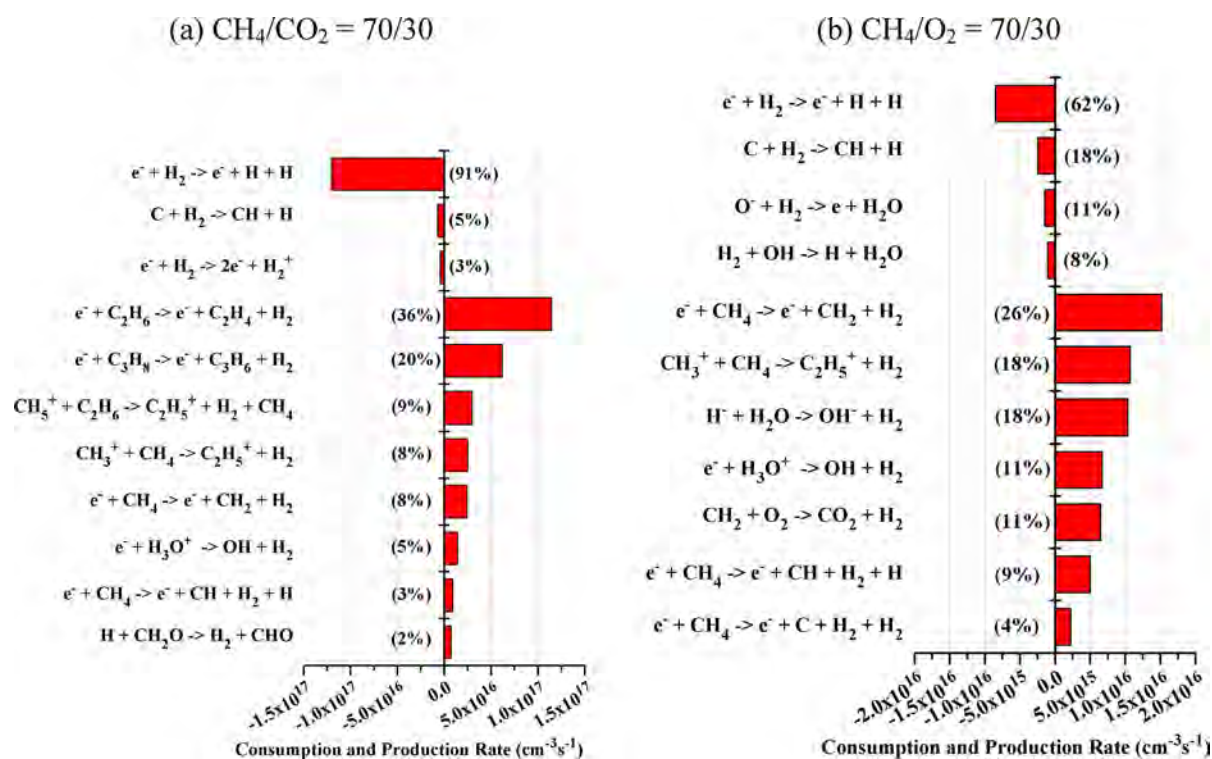


Figure 12. Time-averaged reaction rates of the dominant reaction pathways for the consumption and production of H₂, for a 70/30 CH₄/CO₂ gas mixture (a) and a 70/30 CH₄/O₂ gas mixture (b).

Figure 4a,b, above). The formation and loss mechanisms of the higher hydrocarbon molecules in both gas mixtures are similar to the case of pure CH₄⁹⁴ and will, therefore, not be presented here.

At a higher initial fraction of CO₂, the recombination of CH₃ toward C₂H₆, C₃H₈, and CH₄ will contribute for 57, 22, and 19% to the consumption of CH₃, respectively. On the other hand, at a lower initial fraction of CO₂, the recombination toward C₃H₈ will become more important than the recombination to C₂H₆. In a 90/10 CH₄/O₂ gas mixture, thus a lower O₂ content, the recombination toward C₂H₆ and C₃H₈ becomes more important, with contributions of 38% and 30%, respectively, while the three-body recombination with O₂ molecules, forming CH₃O₂ radicals, contributes for 29% to the consumption of CH₃.

(c). *Formation of Syngas.* In Figure 11a,b, the most important channels for production and loss of CO in a 70/30 CH₄/CO₂ and a 70/30 CH₄/O₂ gas mixture are illustrated, respectively.

As already mentioned above, the reaction of CO₂ with CH₂ radicals is the most important channel for the production of CO in a 70/30 CH₄/CO₂ gas mixture, with a relative contribution of 37% (see Figure 11a). Two other important production mechanisms are the reaction of C₂H₅ with CHO, as well as electron impact dissociation of CO₂, which contribute for 28% and 13% to the total formation of CO in a 70/30 CH₄/CO₂ gas mixture. In the 70/30 CH₄/O₂ gas mixture, on the other hand, 90% of the CO formation occurs through the reaction of O₂ molecules with CHO radicals. It is thus clear that the chemistry yielding CO formation is completely different in both gas mixtures. Note that, in a 20/80 CH₄/CO₂ gas mixture, electron impact dissociation of CO₂ becomes the most important channel for the production of CO.

The same applies to the loss of CO. Indeed, electron impact dissociation and ionization and reactions with H radicals are the most important loss processes for CO in the CH₄/CO₂ gas mixture, while the reaction with OH radicals is the most important loss process for CO in the CH₄/O₂ gas mixture. However, it is clear from Figure 11 that the total rate for CO formation is a factor of 5 and 2.6 higher than the total loss rate, in the CH₄/CO₂ and CH₄/O₂ gas mixtures, respectively.

Figure 12a,b shows the dominant reactions for production and loss of H₂ in a 70/30 CH₄/CO₂ and a 70/30 CH₄/O₂ gas mixture, respectively.

In the 70/30 CH₄/CO₂ gas mixture, electron impact dissociations of C₂H₆ and C₃H₈ are the most important formation channels of H₂, while electron impact dissociation of CH₄ only contributes for 12% (i.e., 8% (toward CH₂ + H₂) + 3% (toward CH + H₂ + H) + 1% (toward C + 2H₂, not shown in Figure 12a). In the 70/30 CH₄/O₂ gas mixture, however, electron impact dissociation of CH₄ is clearly most important. Indeed, the higher hydrocarbons are of lower importance in this case (see Figure 4a,b, above). However, when the initial fraction of O₂ decreases, electron impact dissociations of C₂H₆ and C₃H₈ become the most important formation channels of H₂. Furthermore, electron impact dissociation is the most important loss process for H₂ in both the CH₄/CO₂ and the CH₄/O₂ gas mixtures. In the CH₄/CO₂ mixture, the total loss rate is a factor of 2 lower than the total production rate, while, in the CH₄/O₂ mixture, it is a factor of 4 lower. Nevertheless, the overall H₂ production is still much more pronounced in the CH₄/CO₂ mixture than in the CH₄/O₂ mixture (with a total rate of 1.8 × 10¹⁷ cm⁻³ s⁻¹ vs 4.5 × 10¹⁶ cm⁻³ s⁻¹; see Figure 12), and this explains the higher H₂ density, as well as the higher H₂/CO molar ratio, in the CH₄/CO₂ mixture. The reason for the higher H₂ production in the CH₄/CO₂ mixture is the higher formation of higher hydrocarbons (see above),

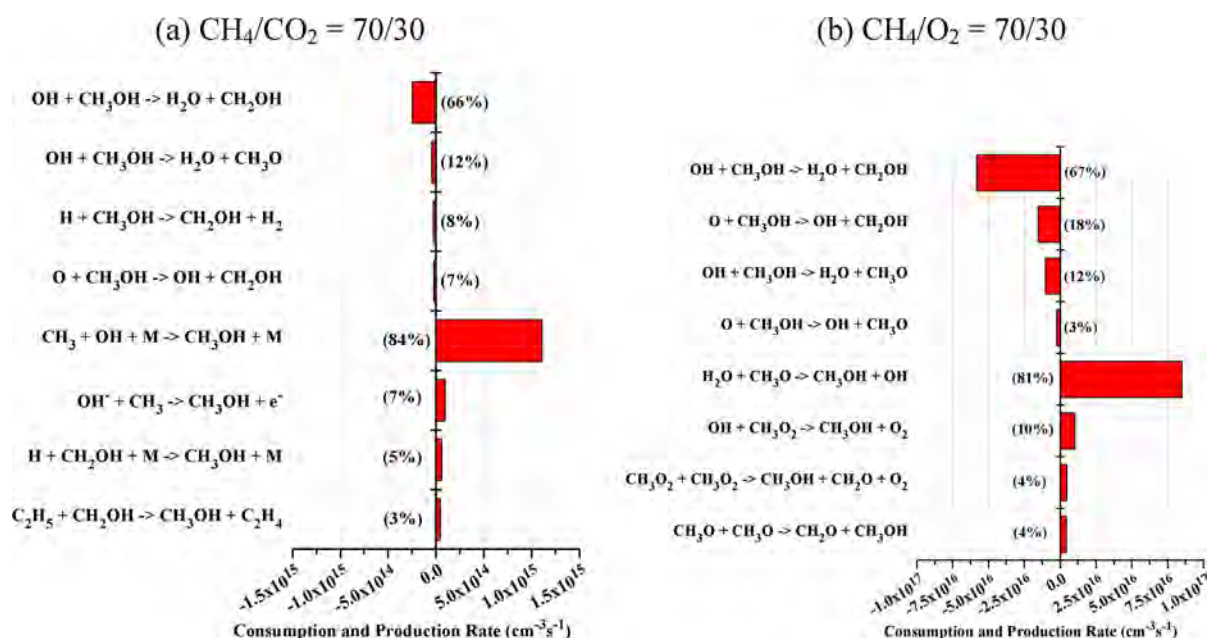


Figure 13. Time-averaged reaction rates of the dominant reaction pathways for the consumption and production of CH_3OH , for a 70/30 CH_4/CO_2 gas mixture (a) and a 70/30 CH_4/O_2 gas mixture (b).

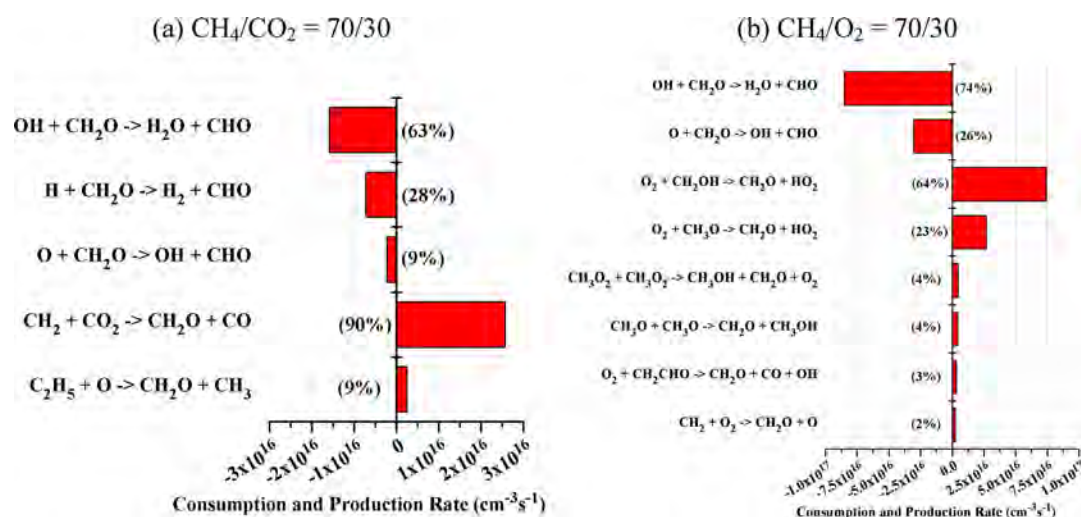


Figure 14. Time-averaged reaction rates of the dominant reaction pathways for the consumption and production of CH_2O , for a 70/30 CH_4/CO_2 gas mixture (a) and a 70/30 CH_4/O_2 gas mixture (b).

which represent additional formation channels for H_2 , as is clear from Figure 12a.

(d). *Formation of Methanol and Formaldehyde.* Figure 13a,b illustrates the dominant reactions for production and loss of CH_3OH in a 70/30 CH_4/CO_2 and a 70/30 CH_4/O_2 gas mixture, respectively, while, in Figure 14a,b, the dominant reactions for production and loss of CH_2O in a 70/30 CH_4/CO_2 and a 70/30 CH_4/O_2 gas mixture are illustrated, respectively.

In the 70/30 CH_4/CO_2 gas mixture, the production of methanol occurs almost entirely through the three-body reaction between the CH_3 and the OH radicals, while, in the 70/30 CH_4/O_2 gas mixture, methanol is almost entirely formed by the reaction between H_2O and CH_3O radicals. Indeed, the rate of the three-body reaction between the CH_3 and the OH radicals is 1 order of magnitude higher in CH_4/CO_2 than in CH_4/O_2 ($1.1 \times 10^{15} \text{ cm}^{-3} \text{ s}^{-1}$ vs $1.6 \times 10^{14} \text{ cm}^{-3} \text{ s}^{-1}$), but the

rate of the reaction between H_2O and CH_3O radicals is 4 orders of magnitude higher in CH_4/O_2 than in CH_4/CO_2 ($8.5 \times 10^{16} \text{ cm}^{-3} \text{ s}^{-1}$ vs $1.4 \times 10^{12} \text{ cm}^{-3} \text{ s}^{-1}$). When comparing the overall production rates in Figure 13, it is clear that the total CH_3OH production rate is almost 2 orders of magnitude higher in the CH_4/O_2 mixture than in the CH_4/CO_2 mixture, explaining the higher CH_3OH density and yield in the CH_4/O_2 mixture (see Figure 4 and Table 2, above).

As already mentioned above, the reaction between CO_2 and CH_2 radicals is the most important channel for the production of formaldehyde in the 70/30 CH_4/CO_2 gas mixture, while, in the 70/30 CH_4/O_2 gas mixture, formaldehyde is mainly produced by the reactions of O_2 with CH_2OH and CH_3O , with relative contributions of 64% and 23%, respectively. The total production rate of CH_2O is a factor of 4 higher in the CH_4/O_2 mixture than in the CH_4/CO_2 mixture, but the total loss rate of CH_2O is a factor of 4.6 higher in the CH_4/O_2

mixture than in the CH₄/CO₂ mixture, explaining the higher CH₂O density and yield in the CH₄/CO₂ mixture (see Figure 4 and Table 2, above).

The most important loss process in both gas mixtures for both methanol and formaldehyde is the reaction with OH radicals. The overall loss rates are again typically lower than the overall production rates.

Note that, for the 70/30 CH₄/O₂ gas mixture, the degradation of methanol leads to the formation of CH₂OH (Figure 13b), which subsequently reacts to formaldehyde (Figure 14b). The degradation of formaldehyde leads to the formation of CHO, which is subsequently converted to CO (Figure 11b). In other words, the formation processes of three of the desired end products (CH₃OH, CH₂O, and CO) are dependent on each other in the 70/30 CH₄/O₂ gas mixture, which is in good agreement with the findings of Larkin et al.²⁴ The development of a catalyst that activates or inhibits one of the reactions influencing the balance between these molecules should make it possible to favor selectively the formation of one of them.

(e). Summary of the Dominant Pathways Governing the Conversion of CH₄ into Higher Oxygenates. Figure 15

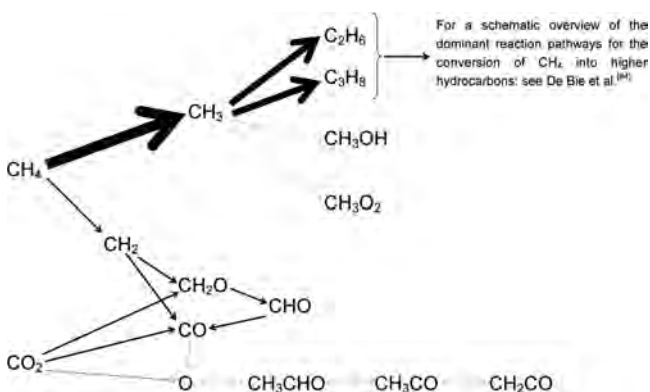


Figure 15. Schematic overview of the dominant reaction pathways for the conversion of CH₄ and CO₂ into higher oxygenates in a 70/30 CH₄/CO₂ gas mixture. The thickness of the arrows is linearly proportional to the rate of the net reaction.

summarizes the dominant reaction pathways for the conversion of CH₄ and CO₂ into higher oxygenates in a 70/30 CH₄/CO₂ gas mixture. The conversion process starts with electron impact dissociation of CH₄, yielding the formation of the CH₃ radicals. The CH₃ radicals will recombine toward higher hydrocarbons, such as C₂H₆ and C₃H₈. Subsequently, a number of dissociation and recombination reactions lead to the conversion toward the other, unsaturated hydrocarbons, and dissociation of CH₄ and the higher hydrocarbons also yields the formation of H₂. The reaction mechanisms toward H₂ and the higher hydrocarbons in the CH₄/CO₂ mixture are exactly the same as in the case of pure CH₄, and thus, more details can be found in De Bie et al.⁹⁴ However, in the CH₄/CO₂ mixture, the CH₃ radicals can also form methanol (CH₃OH) and CH₃O₂ radicals, albeit to a lower extent. Moreover, the CH₂ radicals, which are also formed by electron impact dissociation of CH₄, react with the CO₂ molecules, to form formaldehyde (CH₂O) and CO. Finally, the O atoms, created from electron impact dissociation of CO₂, initiate the formation of other oxygenates, like acetaldehyde (CH₃CHO), which also reacts further into CH₃CO radicals, which can subsequently be converted into ketene (CH₂CO).

However, this reaction path is not so important, because of the limited formation of O radicals compared to CO and CH₂O out of the CO₂ molecules. H₂, CO, ethane (C₂H₆), propene (C₃H₆), and CH₂O are the main end products of the conversion of CH₄ and CO₂ in a 70/30 CH₄/CO₂ gas mixture (see also Figure 4, above).

The dominant reaction pathways for the conversion of CH₄ and O₂ into higher oxygenates in a 70/30 CH₄/O₂ gas mixture are schematically illustrated in Figure 16. Again, electron impact

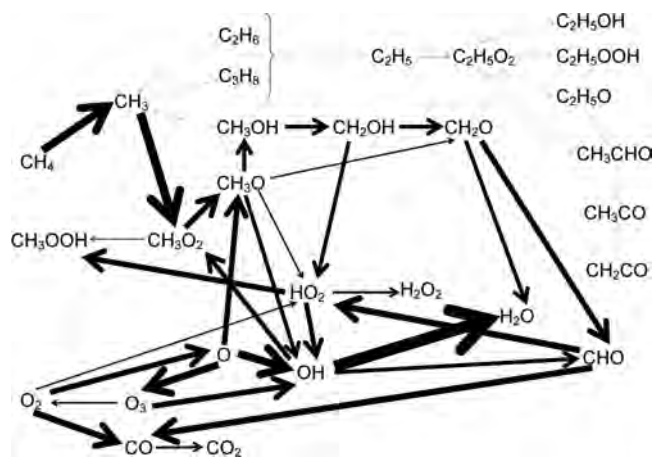


Figure 16. Schematic overview of the dominant reaction pathways for the conversion of CH₄ and O₂ into higher oxygenates in a 70/30 CH₄/O₂ gas mixture. The thickness of the arrows is linearly proportional to the rate of the net reaction.

dissociation of CH₄ results in the formation of CH₃ radicals. The latter can recombine into methanol or higher hydrocarbons, but more important is the recombination into CH₃O₂ radicals, which form either CH₃O radicals or methyl hydroperoxide (CH₃OOH). The CH₃O radicals yield the formation of methanol, which can react further into formaldehyde through the CH₂OH radicals, and formaldehyde can further be converted into CO through the CHO radicals (see above). Furthermore, formaldehyde is also partially converted into water. The O₂ molecules are converted into HO₂ radicals, O atoms, and CO. They are also converted into O₃ molecules, but the O atoms and O₃ molecules quickly react back into O₂ molecules at a somewhat larger rate, so there is a net formation of O₂ molecules out of O₃ (see the direction of the arrow in Figure 16). This delicate balance between O₂, O, and O₃ was also discussed in detail in Aerts et al.¹⁰⁷ CO can be further oxidized into CO₂, which is, of course, undesired. The O atoms are also converted into CH₃O and OH radicals, which can again form water. The most important products in this CH₄/O₂ mixture are H₂O, CO, CO₂, H₂, O₃, CH₃OH, methyl hydroperoxide (CH₃OOH), and hydrogen peroxide (H₂O₂) (see also Figure 4, above). The reaction scheme revealed by our model for the conversion of CH₄ and O₂ into higher oxygenates is in good agreement with the proposed mechanisms for partial oxidation of CH₄ by Goujard et al.⁴¹ and Zhou et al.⁴⁵

4. CONCLUSIONS

In this paper, we have presented the detailed plasma chemistry in a DBD plasma for the conversion of CH₄ in the presence of O₂ or CO₂ into syngas, higher hydrocarbons, and higher oxygenates. We have studied the densities of the various plasma

species as a function of residence time and gas mixing ratio. The spatially averaged densities of the electrons, ions, and radicals exhibit a periodic behavior as a function of time, following the sinusoidal applied voltage, while the spatially averaged molecule densities do not show a periodic behavior. While the densities of some molecules steadily rise as a function of residence time, the densities of other molecules go over a maximum, or show a plateau after some time. This is important to realize, as a careful selection of the residence time can entail a higher production of some targeted molecules. We have also presented the densities of all molecules as a function of the initial gas mixing ratio. The mixtures with CO₂ favor the formation of H₂, CH₂O, CH₃CHO, and CH₂CO, while the densities of H₂O₂, CH₃OH, C₂H₅OH, CH₃OOH, and C₂H₅OOH are higher in the mixtures with O₂. CO is formed at high density in both gas mixtures. Note that, in the gas mixtures with O₂ as coreactant, also a significant amount of undesired CO₂ is formed.

The calculated conversions of the inlet gases as a function of residence time and initial gas mixing ratio are also illustrated. The conversion of CH₄ is roughly independent from the initial O₂ or CO₂ fraction (up to 30–40% CO₂), but it increases for higher initial CO₂ fractions, especially above 70%. The conversions of O₂ and CO₂ both decrease with increasing initial O₂ or CO₂ fraction. However, the O₂ conversion is much higher than the CO₂ conversion.

Finally, the underlying plasma chemistry of the conversion process is analyzed in detail, and the dominant reaction pathways for the consumption of CH₄, O₂, and CO₂ and the production and loss of the dominant end products, i.e., CO, H₂, CH₃OH, and CH₂O, are discussed. Electron impact dissociation of the inlet gases initiates the conversion process. The recombination of CH₃ radicals plays a crucial role, and it was shown that this recombination leads to the formation of higher hydrocarbons in the mixtures with CO₂, while CH₃O₂ radicals are favored in the mixtures with O₂. In the CH₄/CO₂ mixture, also CH₂ radicals play a role, which can be converted into formaldehyde and CO molecules. In the CH₄/O₂ mixture, the CH₃O₂ radicals lead, among others, to the formation of methanol, which can react further into formaldehyde, and the latter can form CO.

Our results are in reasonable agreement with reported results from the literature for similar CH₄/O₂ and CH₄/CO₂ discharges. Moreover, our model provides additional information, mainly on the comparison between the formed end products in CH₄/O₂ and CH₄/CO₂ gas mixtures and on the different pathways leading to these products. In this way, the model can help to determine the most suitable feed gas ratio, residence time, coreactant, and other plasma parameters, to obtain the highest yield and/or selectivity of a desired oxygenates. However, as a lot of different products are typically formed in a plasma, the development of a catalyst, which increases the selective formation of some desired oxygenates, will be crucial. Furthermore, besides the conversion, yield, and selectivity of specific products, also the energy efficiency of the discharge is critical, to determine whether or not plasma technology can compete with conventional technologies.

■ ASSOCIATED CONTENT

● Supporting Information

The Supporting Information is available free of charge on the ACS Publications website at DOI: 10.1021/acs.jpcc.5b06515.

An overview of the reactions included in the model (PDF)

■ AUTHOR INFORMATION

Corresponding Author

*E-mail: annemie.bogaerts@uantwerpen.be. Phone: +32 (0)3 265 2377.

Notes

The authors declare no competing financial interest.

■ ACKNOWLEDGMENTS

This work was carried out using the Turing HPC infrastructure at the CalcUA core facility of the Universiteit Antwerpen, a division of the Flemish Supercomputer Center VSC, funded by the Hercules Foundation, the Flemish Government (department EWI), and the Universiteit Antwerpen. The authors also acknowledge financial support from the IAP/7 (Interuniversity Attraction Pole) program “PSI-Physical Chemistry of Plasma-Surface Interactions” by the Belgian Federal Office for Science Policy (BELSPO) and from the Fund for Scientific Research Flanders (FWO).

■ REFERENCES

- (1) Lunsford, J. H. Catalytic Conversion of Methane to More Useful Chemicals and Fuels: A Challenge for the 21st Century. *Catal. Today* **2000**, *63*, 165–174.
- (2) Aghamir, F. M.; Matin, N. S.; Jalili, A. H.; Esfarayeni, M. H.; Khodagholi, M. A.; Ahmadi, R. Conversion of Methane to Methanol in an AC Dielectric Barrier Discharge. *Plasma Sources Sci. Technol.* **2004**, *13*, 707–711.
- (3) Zou, J. J.; Zhang, Y. P.; Liu, C. J.; Li, Y.; Eliasson, B. Starch-Enhanced Synthesis of Oxygenates from Methane and Carbon Dioxide Using Dielectric-Barrier Discharges. *Plasma Chem. Plasma Process.* **2003**, *23*, 69–82.
- (4) Eliasson, B.; Kogelschatz, U. Modeling and Applications of Silent Discharge Plasmas. *IEEE Trans. Plasma Sci.* **1991**, *19*, 309–323.
- (5) Conrads, H.; Schmidt, M. Plasma Generation and Plasma Sources. *Plasma Sources Sci. Technol.* **2000**, *9*, 441–454.
- (6) Gibalov, V. I.; Pietsch, G. J. The Development of Dielectric Barrier Discharges in Gas Gaps and on Surfaces. *J. Phys. D: Appl. Phys.* **2000**, *33*, 2618–2636.
- (7) Bogaerts, A.; Neyts, E.; Gijbels, R.; van der Mullen, J. Gas Discharge Plasmas and Their Applications. *Spectrochim. Acta, Part B* **2002**, *57*, 609–658.
- (8) Kogelschatz, U. Filamentary, Patterned, and Diffuse Barrier Discharges. *IEEE Trans. Plasma Sci.* **2002**, *30*, 1400–1408.
- (9) Kogelschatz, U. Dielectric-Barrier Discharges: Their History, Discharge Physics, and Industrial Applications. *Plasma Chem. Plasma Process.* **2003**, *23*, 1–46.
- (10) Kogelschatz, U.; Eliasson, B.; Egli, W. From Ozone Generators to Flat Television Screens: History and Future Potential of Dielectric-Barrier Discharges. *Pure Appl. Chem.* **1999**, *71*, 1819–1828.
- (11) Kim, H. H. Nonthermal Plasma Processing for Air-Pollution Control: A Historical Review, Current Issues, and Future Prospects. *Plasma Processes Polym.* **2004**, *1*, 91–110.
- (12) Istadi, I.; Amin, N. A. S. Co-Generation of Synthesis Gas and C₂₊ Hydrocarbons from Methane and Carbon Dioxide in a Hybrid Catalytic-Plasma Reactor: A Review. *Fuel* **2006**, *85*, 577–592.
- (13) Chang, J. S. Physics and Chemistry of Plasma Pollution Control Technology. *Plasma Sources Sci. Technol.* **2008**, *17*, 045004.
- (14) Nozaki, T.; Okazaki, K. Innovative Methane Conversion Technology Using Atmospheric Pressure Non-Thermal Plasma. *J. Jpn. Pet. Inst.* **2011**, *54*, 146–158.
- (15) Matsumoto, H.; Tanabe, S.; Okitsu, K.; Hayashi, Y.; Suib, S. L. Selective Oxidation of Methane to Methanol and Formaldehyde with

Nitrous Oxide in a Dielectric-Barrier Discharge - Plasma Reactor. *J. Phys. Chem. A* **2001**, *105*, 5304–5308.

(16) Rueangjitt, N.; Akarawitoo, C.; Sreethawong, T.; Chavadej, S. Reforming of CO₂-Containing Natural Gas Using an AC Gliding Arc System: Effect of Gas Components in Natural Gas. *Plasma Chem. Plasma Process.* **2007**, *27*, 559–576.

(17) Rueangjitt, N.; Sreethawong, T.; Chavadej, S. Reforming of CO₂-Containing Natural Gas Using an AC Gliding Arc System: Effects of Operational Parameters and Oxygen Addition in Feed. *Plasma Chem. Plasma Process.* **2008**, *28*, 49–67.

(18) Luche, J.; Aubry, O.; Khacef, A.; Cormier, J. M. Syngas Production from Methane Oxidation Using a Non-Thermal Plasma: Experiments and Kinetic Modeling. *Chem. Eng. J.* **2009**, *149*, 35–41.

(19) Huang, L. A.; Zhang, X. W.; Chen, L.; Lei, L. C. Direct Oxidation of Methane to Methanol over Cu-Based Catalyst in an AC Dielectric Barrier Discharge. *Plasma Chem. Plasma Process.* **2011**, *31*, 67–77.

(20) Liu, C. J.; Marafee, A.; Mallinson, R.; Lobban, L. Methane Conversion to Higher Hydrocarbons in a Corona Discharge over Metal Oxide Catalysts with OH Groups. *Appl. Catal., A* **1997**, *164*, 21–33.

(21) Zhou, L. M.; Xue, B.; Kogelschatz, U.; Eliasson, B. Partial Oxidation of Methane to Methanol with Oxygen or Air in a Nonequilibrium Discharge Plasma. *Plasma Chem. Plasma Process.* **1998**, *18*, 375–393.

(22) Larkin, D. W.; Caldwell, T. A.; Lobban, L. L.; Mallinson, R. G. Oxygen Pathways and Carbon Dioxide Utilization in Methane Partial Oxidation in Ambient Temperature Electric Discharges. *Energy Fuels* **1998**, *12*, 740–744.

(23) Okumoto, M.; Mizuno, A. Conversion of Methane for Higher Hydrocarbon Fuel Synthesis Using Pulsed Discharge Plasma Method. *Catal. Today* **2001**, *71*, 211–217.

(24) Larkin, D. W.; Zhou, L. M.; Lobban, L. L.; Mallinson, R. G. Product Selectivity Control and Organic Oxygenate Pathways from Partial Oxidation of Methane in a Silent Electric Discharge Reactor. *Ind. Eng. Chem. Res.* **2001**, *40*, 5496–5506.

(25) Larkin, D. W.; Lobban, L. L.; Mallinson, R. G. Production of Organic Oxygenates in the Partial Oxidation of Methane in a Silent Electric Discharge Reactor. *Ind. Eng. Chem. Res.* **2001**, *40*, 1594–1601.

(26) Larkin, D. W.; Lobban, L. L.; Mallinson, R. G. The Direct Partial Oxidation of Methane to Organic Oxygenates Using a Dielectric Barrier Discharge Reactor as a Catalytic Reactor Analog. *Catal. Today* **2001**, *71*, 199–210.

(27) Okumoto, M.; Kim, H. H.; Takashima, K.; Katsura, S.; Mizuno, A. Reactivity of Methane in Nonthermal Plasma in the Presence of Oxygen and Inert Gases at Atmospheric Pressure. *IEEE Trans. Ind. Appl.* **2001**, *37*, 1618–1624.

(28) Cho, W.; Baek, Y.; Moon, S. K.; Kim, Y. C. Oxidative Coupling of Methane with Microwave and RF Plasma Catalytic Reaction over Transitional Metals Loaded on ZSM-5. *Catal. Today* **2002**, *74*, 207–223.

(29) Pietruszka, B.; Anklam, K.; Heintze, M. Plasma-Assisted Partial Oxidation of Methane to Synthesis Gas in a Dielectric Barrier Discharge. *Appl. Catal., A* **2004**, *261*, 19–24.

(30) Heintze, M.; Pietruszka, B. Plasma Catalytic Conversion of Methane into Syngas: The Combined Effect of Discharge Activation and Catalysis. *Catal. Today* **2004**, *89*, 21–25.

(31) Nozaki, T.; Hattori, A.; Okazaki, K. Partial Oxidation of Methane Using a Microscale Non-Equilibrium Plasma Reactor. *Catal. Today* **2004**, *98*, 607–616.

(32) Indarto, A.; Choi, J.-W.; Lee, H.; Song, H. K.; Palgunadi, J. Partial Oxidation of Methane with Sol-Gel Fe/Hf/YSZ Catalyst in Dielectric Barrier Discharge: Catalyst Activation by Plasma. *J. Rare Earths* **2006**, *24*, 513–518.

(33) Sreethawong, T.; Thakonpatthanakun, P.; Chavadej, S. Partial Oxidation of Methane with Air for Synthesis Gas Production in a Multistage Gliding Arc Discharge System. *Int. J. Hydrogen Energy* **2007**, *32*, 1067–1079.

(34) Nair, S. A.; Nozaki, T.; Okazaki, K. Methane Oxidative Conversion Pathways in a Dielectric Barrier Discharge Reactor - Investigation of Gas Phase Mechanism. *Chem. Eng. J.* **2007**, *132*, 85–95.

(35) Indarto, A.; Lee, H.; Choi, J. W.; Song, H. K. Partial Oxidation of Methane with Yttria-Stabilized Zirconia Catalyst in a Dielectric Barrier Discharge. *Energy Sources, Part A* **2008**, *30*, 1628–1636.

(36) Indarto, A.; Yang, D. R.; Palgunadi, J.; Choi, J. W.; Lee, H.; Song, H. K. Partial Oxidation of Methane with Cu-Zn-Al Catalyst in a Dielectric Barrier Discharge. *Chem. Eng. Process.* **2008**, *47*, 780–786.

(37) Matin, N. S.; Savadkoobi, H. A.; Feizabadi, S. Y. Methane Conversion to C-2 Hydrocarbons Using Dielectric-Barrier Discharge Reactor: Effects of System Variables. *Plasma Chem. Plasma Process.* **2008**, *28*, 189–202.

(38) Wang, B. W.; Zhang, X.; Liu, Y. W.; Xu, G. H. Conversion of CH₄, Steam and O₂ to Syngas and Hydrocarbons Via Dielectric Barrier Discharge. *J. Nat. Gas Chem.* **2009**, *18*, 94–97.

(39) Nozaki, T.; Ağiral, A.; Yuzawa, S.; Han Gardeniers, J. G. E.; Okazaki, K. A Single Step Methane Conversion into Synthetic Fuels Using Microplasma Reactor. *Chem.—Eng. J.* **2011**, *166*, 288–293.

(40) Nozaki, T.; Goujard, V.; Yuzawa, S.; Moriyama, S.; Ağiral, A.; Okazaki, K. Selective Conversion of Methane to Synthetic Fuels Using Dielectric Barrier Discharge Contacting Liquid Film. *J. Phys. D: Appl. Phys.* **2011**, *44*, 274010.

(41) Goujard, V.; Nozaki, T.; Yuzawa, S.; Ağiral, A.; Okazaki, K. Plasma-Assisted Partial Oxidation of Methane at Low Temperatures: Numerical Analysis of Gas-Phase Chemical Mechanism. *J. Phys. D: Appl. Phys.* **2011**, *44*, 274011.

(42) Ağiral, A.; Nozaki, T.; Nakase, M.; Yuzawa, S.; Okazaki, K.; (Han) Gardeniers, J. G. E. Gas-to-Liquids Process Using Multi-Phase Flow, Non-Thermal Plasma Microreactor. *Chem.—Eng. J.* **2011**, *167*, 560–566.

(43) Zhou, J.; Xu, Y.; Zhou, X.; Gong, J.; Yin, Y.; Zheng, H.; Guo, H. Direct Oxidation of Methane to Hydrogen Peroxide and Organic Oxygenates in a Double Dielectric Plasma Reactor. *ChemSusChem* **2011**, *4*, 1095–1098.

(44) Zhou, L. M.; Xue, B.; Kogelschatz, U.; Eliasson, B. Non-equilibrium Plasma Reforming of Greenhouse Gases to Synthesis Gas. *Energy Fuels* **1998**, *12*, 1191–1199.

(45) Huang, A. M.; Xia, G. G.; Wang, J. Y.; Suib, S. L.; Hayashi, Y.; Matsumoto, H. CO₂ Reforming of CH₄ by Atmospheric Pressure AC Discharge Plasmas. *J. Catal.* **2000**, *189*, 349–359.

(46) Kozlov, K. V.; Michel, P.; Wagner, H. E. Synthesis of Organic Compounds from Mixtures of Methane with Carbon Dioxide in Dielectric-Barrier Discharges at Atmospheric Pressure. *Plasmas Polym.* **2000**, *5*, 129–150.

(47) Eliasson, B.; Liu, C. J.; Kogelschatz, U. Direct Conversion of Methane and Carbon Dioxide to Higher Hydrocarbons Using Catalytic Dielectric-Barrier Discharges with Zeolites. *Ind. Eng. Chem. Res.* **2000**, *39*, 1221–1227.

(48) Yao, S. L.; Ouyang, F.; Nakayama, A.; Suzuki, E.; Okumoto, N.; Mizuno, A. Oxidative Coupling and Reforming of Methane with Carbon Dioxide Using a High-Frequency Pulsed Plasma. *Energy Fuels* **2000**, *14*, 910–914.

(49) Zhang, K.; Kogelschatz, U.; Eliasson, B. Conversion of Greenhouse Gases to Synthesis Gas and Higher Hydrocarbons. *Energy Fuels* **2001**, *15*, 395–402.

(50) Kraus, M.; Eliasson, B.; Kogelschatz, U.; Wokaun, A. CO₂ Reforming of Methane by the Combination of Dielectric-Barrier Discharges and Catalysis. *Phys. Chem. Chem. Phys.* **2001**, *3*, 294–300.

(51) Liu, C. J.; Xue, B. Z.; Eliasson, B.; He, F.; Li, Y.; Xu, G. H. Methane Conversion to Higher Hydrocarbons in the Presence of Carbon Dioxide Using Dielectric-Barrier Discharge Plasmas. *Plasma Chem. Plasma Process.* **2001**, *21*, 301–310.

(52) Yao, S. L.; Okumoto, M.; Nakayama, A.; Suzuki, E. Plasma Reforming and Coupling of Methane with Carbon Dioxide. *Energy Fuels* **2001**, *15*, 1295–1299.

- (53) Jiang, T.; Li, Y.; Liu, C. J.; Xu, G. H.; Eliasson, B.; Xue, B. Z. Plasma Methane Conversion Using Dielectric-Barrier Discharges with Zeolite A. *Catal. Today* **2002**, *72*, 229–235.
- (54) Zhang, X. L.; Dai, B.; Zhu, A. M.; Gong, W. M.; Liu, C. H. The Simultaneous Activation of Methane and Carbon Dioxide to C₂ Hydrocarbons under Pulse Corona Plasma over La₂O₃/gamma-Al₂O₃ Catalyst. *Catal. Today* **2002**, *72*, 223–227.
- (55) Zhang, K.; Eliasson, B.; Kogelschatz, U. Direct Conversion of Greenhouse Gases to Synthesis Gas and C₄ Hydrocarbons over Zeolite HY Promoted by a Dielectric-Barrier Discharge. *Ind. Eng. Chem. Res.* **2002**, *41*, 1462–1468.
- (56) Li, Y.; Liu, C. J.; Eliasson, B.; Wang, Y. Synthesis of Oxygenates and Higher Hydrocarbons Directly from Methane and Carbon Dioxide Using Dielectric-Barrier Discharges: Product Distribution. *Energy Fuels* **2002**, *16*, 864–870.
- (57) Hwang, B.; Yeo, Y.; Na, B. Conversion of CH₄ and CO₂ to Syngas and Higher Hydrocarbons Using Dielectric Barrier Discharge. *Korean J. Chem. Eng.* **2003**, *20*, 631–634.
- (58) Zhang, Y. P.; Li, Y.; Wang, Y.; Liu, C. J.; Eliasson, B. Plasma Methane Conversion in the Presence of Carbon Dioxide Using Dielectric-Barrier Discharges. *Fuel Process. Technol.* **2003**, *83*, 101–109.
- (59) Zhang, J. Q.; Zhang, J. S.; Yang, Y. J.; Liu, Q. Oxidative Coupling and Reforming of Methane with Carbon Dioxide Using a Pulsed Microwave Plasma under Atmospheric Pressure. *Energy Fuels* **2003**, *17*, 54–59.
- (60) Song, H. K.; Choi, J. W.; Yue, S. H.; Lee, H.; Na, B. K. Synthesis Gas Production Via Dielectric Barrier Discharge over Ni/gamma-Al₂O₃ Catalyst. *Catal. Today* **2004**, *89*, 27–33.
- (61) Song, H. K.; Lee, H.; Choi, J.-W.; Na, B.-k. Effect of Electrical Pulse Forms on the CO₂ Reforming of Methane Using Atmospheric Dielectric Barrier Discharge. *Plasma Chem. Plasma Process.* **2004**, *24*, 57–72.
- (62) Indarto, A.; Choi, J.-W.; Lee, H.; Song, H. K. Effect of Additive Gases on Methane Conversion Using Gliding Arc Discharge. *Energy* **2006**, *31*, 2986–2995.
- (63) Li, M. W.; Tian, Y. L.; Xu, G. H. Characteristics of Carbon Dioxide Reforming of Methane Via Alternating Current (AC) Corona Plasma Reactions. *Energy Fuels* **2007**, *21*, 2335–2339.
- (64) Li, D. H.; Li, X.; Bai, M. G.; Tao, X. M.; Shang, S. Y.; Dai, X. Y.; Yin, Y. X. CO₂ Reforming of CH₄ by Atmospheric Pressure Glow Discharge Plasma: A High Conversion Ability. *Int. J. Hydrogen Energy* **2009**, *34*, 308–313.
- (65) Wang, Q.; Yan, B. H.; Jin, Y.; Cheng, Y. Dry Reforming of Methane in a Dielectric Barrier Discharge Reactor with Ni/Al₂O₃ Catalyst: Interaction of Catalyst and Plasma. *Energy Fuels* **2009**, *23*, 4196–4201.
- (66) Wang, Q.; Yan, B. H.; Jin, Y.; Cheng, Y. Investigation of Dry Reforming of Methane in a Dielectric Barrier Discharge Reactor. *Plasma Chem. Plasma Process.* **2009**, *29*, 217–228.
- (67) Wang, Q.; Cheng, Y.; Jin, Y. Dry Reforming of Methane in an Atmospheric Pressure Plasma Fluidized Bed with Ni/gamma-Al₂O₃ Catalyst. *Catal. Today* **2009**, *148*, 275–282.
- (68) Sentek, J.; Krawczyk, K.; Mlotek, M.; Kalczevska, M.; Kroker, T.; Kolb, T.; Schenk, A.; Gericke, K. H.; Schmidt-Szalowski, K. Plasma-Catalytic Methane Conversion with Carbon Dioxide in Dielectric Barrier Discharges. *Appl. Catal., B* **2010**, *94*, 19–26.
- (69) Seyed-Matin, N.; Jalili, A. H.; Jenab, M. H.; Zekordi, S. M.; Afzali, A.; Rasouli, C.; Zamaniyan, A. DC-Pulsed Plasma for Dry Reforming of Methane to Synthesis Gas. *Plasma Chem. Plasma Process.* **2010**, *30*, 333–347.
- (70) Yan, B. H.; Wang, Q.; Jin, Y.; Cheng, Y. Dry Reforming of Methane with Carbon Dioxide Using Pulsed DC Arc Plasma at Atmospheric Pressure. *Plasma Chem. Plasma Process.* **2010**, *30*, 257–266.
- (71) Rico, V. J.; Hueso, J. L.; Cotrino, J.; Gonzalez-Elipse, A. R. Evaluation of Different Dielectric Barrier Discharge Plasma Configurations as an Alternative Technology for Green C₁ Chemistry in the Carbon Dioxide Reforming of Methane and the Direct Decomposition of Methanol. *J. Phys. Chem. A* **2010**, *114*, 4009–4016.
- (72) Scarduelli, G.; Guella, G.; Ascenzi, D.; Tosi, P. Synthesis of Liquid Organic Compounds from CH₄ and CO₂ in a Dielectric Barrier Discharge Operating at Atmospheric Pressure. *Plasma Processes Polym.* **2011**, *8*, 25–31.
- (73) Machrafi, H.; Cavadias, S.; Amouroux, J. CO₂ Valorization by Means of Dielectric Barrier Discharge. *J. Phys.: Conf. Ser.* **2011**, *275*, 012016.
- (74) Pinhão, N. R.; Janeco, A.; Branco, J. B. Influence of Helium on the Conversion of Methane and Carbon Dioxide in a Dielectric Barrier Discharge. *Plasma Chem. Plasma Process.* **2011**, *31*, 427–439.
- (75) Tu, X.; Gallon, H. J.; Twigg, M. V.; Gorry, P. A.; Whitehead, J. C. Dry Reforming of Methane over a Ni/Al₂O₃ Catalyst in a Coaxial Dielectric Barrier Discharge Reactor. *J. Phys. D: Appl. Phys.* **2011**, *44*, 274007.
- (76) Goujard, V.; Tatibouet, J. M.; Batiot-Dupeyrat, C. Carbon Dioxide Reforming of Methane Using a Dielectric Barrier Discharge Reactor: Effect of Helium Dilution and Kinetic Model. *Plasma Chem. Plasma Process.* **2011**, *31*, 315–325.
- (77) Schmidt-Szalowski, K.; Krawczyk, K.; Sentek, J.; Ulejczyk, B.; Gorska, A.; Mlotek, M. Hybrid Plasma-Catalytic Systems for Converting Substances of High Stability, Greenhouse Gases and VOC. *Chem. Eng. Res. Des.* **2011**, *89*, 2643–2651.
- (78) Wang, Q.; Shi, H. L.; Yan, B. H.; Jin, Y.; Cheng, Y. Steam Enhanced Carbon Dioxide Reforming of Methane in DBD Plasma Reactor. *Int. J. Hydrogen Energy* **2011**, *36*, 8301–8306.
- (79) Gallon, H. J.; Tu, X.; Whitehead, J. C. Effects of Reactor Packing Materials on H₂ Production by CO₂ Reforming of CH₄ in a Dielectric Barrier Discharge. *Plasma Processes Polym.* **2012**, *9*, 90–97.
- (80) Kim, T. K.; Lee, W. G. Reaction between Methane and Carbon Dioxide to Produce Syngas in Dielectric Barrier Discharge System. *J. Ind. Eng. Chem.* **2012**, *18*, 1710–1714.
- (81) Kolb, T.; Kroker, T.; Voigt, J. H.; Gericke, K. H. Wet Conversion of Methane and Carbon Dioxide in a DBD Reactor. *Plasma Chem. Plasma Process.* **2012**, *32*, 1139–1155.
- (82) Tu, X.; Whitehead, J. C. Plasma-Catalytic Dry Reforming of Methane in an Atmospheric Dielectric Barrier Discharge: Understanding the Synergistic Effect at Low Temperature. *Appl. Catal., B* **2012**, *125*, 439–448.
- (83) Liu, C. J.; Mallinson, R.; Lobban, L. Nonoxidative Methane Conversion to Acetylene over Zeolite in a Low Temperature Plasma. *J. Catal.* **1998**, *179*, 326–334.
- (84) Gordon, C. L.; Lobban, L. L.; Mallinson, R. G. Ethylene Production Using a Pd and Ag-Pd-Y-Zeolite Catalyst in a DC Plasma Reactor. *Catal. Today* **2003**, *84*, 51–57.
- (85) Nozaki, T.; Muto, N.; Kadio, S.; Okazaki, K. Dissociation of Vibrationally Excited Methane on Ni Catalyst - Part 2. Process Diagnostics by Emission Spectroscopy. *Catal. Today* **2004**, *89*, 67–74.
- (86) Snoeckx, R.; Setareh, M.; Aerts, R.; Simon, P.; Maghari, A.; Bogaerts, A. Influence of N₂ Concentration in a CH₄/N₂ Dielectric Barrier Discharge Used for CH₄ Conversion into H₂. *Int. J. Hydrogen Energy* **2013**, *38*, 16098–16120.
- (87) Bugaev, S. P.; Kozyrev, A. V.; Kuvshinov, V. A.; Sochugov, N. S.; Khryapov, P. A. Plasma-Chemical Conversion of Lower Alkanes with Stimulated Condensation of Incomplete Oxidation Products. *Plasma Chem. Plasma Process.* **1998**, *18*, 247–261.
- (88) Kraus, M.; Egli, W.; Haffner, K.; Eliasson, B.; Kogelschatz, U.; Wokaun, A. Investigation of Mechanistic Aspects of the Catalytic CO₂ Reforming of Methane in a Dielectric-Barrier Discharge Using Optical Emission Spectroscopy and Kinetic Modeling. *Phys. Chem. Chem. Phys.* **2002**, *4*, 668–675.
- (89) Matin, N. S.; Whitehead, J. C. A Chemical Model for the Atmospheric Pressure Plasma Reforming of Methane with Oxygen. In *28th ICPIG*, Prague, Czech Republic, July 15–20, 2007; Institute of Plasma Physics: Prague, Czech Republic, 2007; pp 983–986.
- (90) Snoeckx, R.; Aerts, R.; Tu, X.; Bogaerts, A. Plasma-Based Dry Reforming: A Computational Study Ranging from the Nanoseconds to Seconds Time Scale. *J. Phys. Chem. C* **2013**, *117*, 4957–4970.

(91) Snoeckx, R.; Zeng, Y. X.; Tu, X.; Bogaerts, A. Plasma-Based Dry Reforming: Improving the Conversion and Energy Efficiency in a Dielectric Barrier Discharge. *RSC Adv.* **2015**, *5*, 29799–29808.

(92) Wang, J. G.; Liu, C. J.; Eliasson, B. Density Functional Theory Study of Synthesis of Oxygenates and Higher Hydrocarbons from Methane and Carbon Dioxide Using Cold Plasmas. *Energy Fuels* **2004**, *18*, 148–153.

(93) Istadi, I.; Amin, N. A. S. Modelling and Optimization of Catalytic-Dielectric Barrier Discharge Plasma Reactor for Methane and Carbon Dioxide Conversion Using Hybrid Artificial Neural Network - Genetic Algorithm Technique. *Chem. Eng. Sci.* **2007**, *62*, 6568–6581.

(94) De Bie, C.; Verheyde, B.; Martens, T.; van Dijk, J.; Paulussen, S.; Bogaerts, A. Fluid Modeling of the Conversion of Methane into Higher Hydrocarbons in an Atmospheric Pressure Dielectric Barrier Discharge. *Plasma Processes Polym.* **2011**, *8*, 1033–1058.

(95) van Dijk, J.; Peerenboom, K.; Jimenez, M.; Mihailova, D.; van der Mullen, J. The Plasma Modelling Toolkit Plasimo. *J. Phys. D: Appl. Phys.* **2009**, *42*, 194012.

(96) <http://plasimo.phys.tue.nl>.

(97) Hagelaar, G. J. M. Modeling of Microdischarges for Display Technology. Ph.D. Thesis, Eindhoven University of Technology, Eindhoven, The Netherlands, 2000.

(98) Brok, W. J. M.; van Dijk, J.; Bowden, M. D.; van der Mullen, J. J. A. M.; Kroesen, G. M. W. A Model Study of Propagation of the First Ionization Wave During Breakdown in a Straight Tube Containing Argon. *J. Phys. D: Appl. Phys.* **2003**, *36*, 1967–1979.

(99) Herrebout, D.; Bogaerts, A.; Yan, M.; Gijbels, R.; Goedheer, W.; Dekempeneer, E. One-Dimensional Fluid Model for an RF Methane Plasma of Interest in Deposition of Diamond-Like Carbon Layers. *J. Appl. Phys.* **2001**, *90*, 570–579.

(100) Farouk, T.; Farouk, B.; Gutsol, A.; Fridman, A. Atmospheric Pressure Methane-Hydrogen DC Micro-Glow Discharge for Thin Film Deposition. *J. Phys. D: Appl. Phys.* **2008**, *41*, 175202.

(101) Hagelaar, G. J. M.; Pitchford, L. C. Solving the Boltzmann Equation to Obtain Electron Transport Coefficients and Rate Coefficients for Fluid Models. *Plasma Sources Sci. Technol.* **2005**, *14*, 722–733.

(102) Paulussen, S.; Verheyde, B.; Tu, X.; De Bie, C.; Martens, T.; Petrovic, D.; Bogaerts, A.; Sels, B. Conversion of Carbon Dioxide to Value-Added Chemicals in Atmospheric Pressure Dielectric Barrier Discharges. *Plasma Sources Sci. Technol.* **2010**, *19*, 034015.

(103) Book, N. L.; Sitton, O. C.; Ludlow, D. K. *Inerting or Purging*; University of Missouri-Rolla: Rollam, MO, 2000.

(104) Lawton, S. A.; Phelps, A. V. Excitation of B1-Sigma-G+ State of O₂ by Low-Energy Electrons. *J. Chem. Phys.* **1978**, *69*, 1055–1068.

(105) Eliasson, B.; Hirth, M.; Kogelschatz, U. Ozone Synthesis from Oxygen in Dielectric Barrier Discharges. *J. Phys. D: Appl. Phys.* **1987**, *20*, 1421–1437.

(106) Itikawa, Y. Cross Sections for Electron Collisions with Carbon Dioxide. *J. Phys. Chem. Ref. Data* **2002**, *31*, 749–767.

(107) Aerts, R.; Somers, W.; Bogaerts, A. Carbon Dioxide Splitting in a Dielectric Barrier Discharge Plasma: A Combined Experimental and Computational Study. *ChemSusChem* **2015**, *8*, 702–716.